



**NTNU – Trondheim**  
Norwegian University of  
Science and Technology

# Simulation of Marine Lifting Operations with Focus on Structural Response Control

**Arild Eriksen Matland**

Marine Technology

Submission date: June 2014

Supervisor: Jørgen Amdahl, IMT

Norwegian University of Science and Technology  
Department of Marine Technology



MASTER THESIS 2014

for

Stud. Techn. Arild Matland

**Simulation of Marine Lifting Operations with Focus on Structural Response Control**  
*Simulering av marine løfteoperasjoner med fokus på kontroll av konstruksjonsrepons*

Offshore oil and gas activities move steadily into deeper waters and harsher environment. Subsea installations become more and more common for extraction of hydrocarbons. This development puts heavy demands on contractors for them to be able to perform safe and efficient installations, inspections and interventions. At present, many operations require benign environmental conditions and are thus limited to the summer period. Time constraints may be by increased efficiency, i.e. by reduction of time for each individual operation. Alternatively, the weather window may be increased, by increasing the limiting significant wave height for operation. In either case the structural load effects may increase, and proper control of the structural response is prerequisite. Lift off, motion through the splash zone and landing of the equipment are especially challenging. Feedback from structural response to the control loop may contribute to reducing the load effects in these phases. The hydrodynamics loads may not be very well known or properly implemented in software used for analysis of the marine operations. Additionally the resistance formulas may not be adequate if impulsive type actions are encountered.

The purpose of the work is to assess the applicability of USFOS and possibly alternative software to simulate selected lift operations. Focus will be placed on code checking of structural response histories. The work is proposed to be carried out in the following steps:

- 1) Review of various subsea installations and equipment that will be installed by lift operations. Discuss the expected load conditions that will be encountered and potential failure modes that must be controlled. From this overview, select the scenarios that will be investigated by simulation. It is suggested that focus is put on installations and equipment where Morrison forces and slamming forces are important.
- 2) A briefed review of alternative software for simulation of the selected scenarios (e.g. SIMO/RIFEX)
- 3) Familiarise with USFOS for modelling the lifting behaviour by establishing a very simple, idealised model. The starting point is the given finite element model.
- 4) Establish the finite element model in USFOS for the cases selected for analysis. The model will include the installation/equipment, the wires and the crane. The lifting vessel/barge may be modelled as a two-node element, with one node in the centre of gravity. The

vessel motions may be simulated on the basis of transfer functions for wave induced displacement, or wave forces for various incoming wave angles.

- 5) Establish finite element models for simulations with alternative software.
- 6) Perform simulation of the lifting operations for the selected scenarios. This may comprise both lift off, through the splash zone and landing on sea floor. The environmental conditions shall be varied. Extreme load cases shall be sought. Of particular interest may be intense, short duration load pulses caused by wave slamming or contact forces during landing. Evaluate the risk of yielding or buckling according to API RP2A WSD by utility tool for code checking of structural response. Discuss also if dynamic buckling may need to be considered. To facilitate large parametric variations it should be considered to automatize these simulations by using scripts.
- 7) For a few cases perform analysis with alternative software and to the extent possible compare the results with those obtained with USFOS.
- 8) On the basis of the experience obtained in pt. 6 and 7 discuss the appropriateness of the tools for simulations of marine operations. Discuss challenges that may need to be resolved. Conclusions and recommendations for further work

Literature studies of specific topics relevant to the thesis work may be included.

The work scope may prove to be larger than initially anticipated. Subject to approval from the supervisors, topics may be deleted from the list above or reduced in extent.

In the thesis the candidate shall present his personal contribution to the resolution of problems within the scope of the thesis work.

Theories and conclusions should be based on mathematical derivations and/or logic reasoning identifying the various steps in the deduction.

The candidate should utilise the existing possibilities for obtaining relevant literature.

### **Thesis format**

The thesis should be organised in a rational manner to give a clear exposition of results, assessments, and conclusions. The text should be brief and to the point, with a clear language. Telegraphic language should be avoided.

The thesis shall contain the following elements: A text defining the scope, preface, list of contents, summary, main body of thesis, conclusions with recommendations for further work, list of symbols and acronyms, references and (optional) appendices. All figures, tables and equations shall be numerated.

The supervisors may require that the candidate, in an early stage of the work, presents a written plan for the completion of the work. The plan should include a budget for the use of computer and laboratory resources which will be charged to the department. Overruns shall be reported to the supervisors.



The original contribution of the candidate and material taken from other sources shall be clearly defined. Work from other sources shall be properly referenced using an acknowledged referencing system.

The report shall be submitted in two copies:

- Signed by the candidate
- The text defining the scope included
- In bound volume(s)
- Drawings and/or computer prints which cannot be bound should be organised in a separate folder.
- The report shall also be submitted in pdf format along with essential input files for computer analysis, spreadsheets, MATLAB files etc in digital format.
- 

### **Ownership**

NTNU has according to the present rules the ownership of the thesis. Any use of the thesis has to be approved by NTNU (or external partner when this applies). The department has the right to use the thesis as if the work was carried out by a NTNU employee, if nothing else has been agreed in advance.

### **Thesis supervisor**

Prof. Jørgen Amdahl

**Deadline: June 10, 2014**

Trondheim, January 14, 2014



Jørgen Amdahl



# Preface

This master thesis marks the end of 5 years as a M.Sc student in Marine Technology at NTNU. The work was conducted during the spring semester 2014 under the supervision of Professor Jørgen Amdahl.

Initially the work was intended to cover analyses using two computer programs, USFOS and SIMO, to model marine lifting operations. But due to the workload, it was decided that the focus should be put on USFOS. Because the latter is not initially made for this application, understanding how to best model operations and interpret the results, have been time consuming. However, it has been interesting to test the limitations of the program.

I would like to thank my supervisor Jørgen Amdahl for proposing the thesis work and for guidance throughout the semester. A thanks is also given to Tore Holmås, who have been very helpful with USFOS related problems that have arisen.

In addition to this, a special thanks is given to the people at office A 1.027 for help and discussion during the work on the thesis.



---

Arild E. Matland  
Tyholt, 10/06/2014





# Summary

As the offshore industry operates on deeper seas, subsea technology becomes more and more important. As a consequence of this, marine lifting operations of subsea equipment has become very common. Prior to such an operation it is necessary to define the limiting sea states. Many methods for doing this are very conservative and will underestimate the operational conditions. Defining the limiting sea states can be done by numerical simulations using commercial software. However this may be very time consuming.

The focus on this report is put on modeling lifting of objects through the splash zone using the computer program USFOS. Dynamic analyses of the lowering were performed. Even though this program is not initially intended for such use, it has features that makes such analyses possible. In this report the applicability of USFOS for such use will be studied.

Three main models have been considered. The first of them was a very simple model of a horizontal pipe that was lowered into the sea. The wire forces was considered, and it was studied how different input parameters affected the results.

The input parameters for this simple model was taken further by simulating the lowering of a subsea spool through the splash zone. This model consisted of a subsea spool, a spreader bar, 4 slings and a lifting wire. Both flat sea and regular waves were simulated. For the regular wave cases, the forces in the wires and slings was studied. This showed that slack in the lifting wire or slings would occur in 3 out of 4 sea states. Further the elastic utilization of the structure was evaluated according to API-RP-2A-WSD, which is implemented in USFOS. In this study it was found that the utilization of the structure increases as the wave height increases. However it is questioned how accurately USFOS calculates the forces in the splash zone for the most extreme cases of regular waves.

The last and most realistic model that was considered in this thesis, was lowering of the subsea spool into irregular waves. These waves were simulated according to the JONSWAP wave spectrum. Different sea states were modeled by changing the value of significant wave height and peak period. In addition the top end of the lifting wire was connected to the moving crane tip of a vessel. The vessel motions were defined by RAO functions that were included in the input files. For all of the sea states that were modeled, the minimum wire forces were found. This resulted in an overview of which sea states that would give slack in lifting wire or slings. The trend showed that as the significant wave height was increased, the minimum forces in the wires and slings decreased.

From the work that was carried out it was concluded that USFOS can be used for modeling simple marine lifting operations. The program calculates the equilibrium forces in the top end of the wire element in the right way. But its use for this purpose is limited. If damping is introduced to the system, the force in the wire element will decrease due to this, and thus give an error in the equilibrium value. Further the special beam formulation used to model the elongating wire element, requires that a dynamic analysis is performed. Thus there will be oscillations in the system due to initiation of gravity and self weight. Therefore this initial phase should be neglected when considering the structural response.

One of the advantages of the program for this type of use, is its ability to evaluate non-linear structural behavior, and calculate elastic utilization of the structure. There are, however, uncertainties in the elastic utilization calculations when it comes to definitions of parameters such as buckling length.

# Sammendrag

Offshore-industrien opererer stadig på dypere vann. I forbindelse med dette blir undervannsteknologi mer og mer viktig. Dette betyr igjen at marine løfteoperasjoner av undervannsutstyr er svært vanlig. Før en slik operasjon er det nødvendig å definere de begrensende sjøtilstandene for operasjonen. Mange metoder for å gjøre dette er veldig konservative, og vil føre til et redusert vær-vindu for operasjonen. For å definere de begrensende sjøtilstandene kan numeriske analyser ved bruk av kommersiell programvare benyttes. Dette kan imidlertid være svært tidkrevende.

Fokuset i denne rapporten er lagt på å modellere løfting gjennom bølgesonen ved bruk av programmet USFOS. Dynamiske analyser av senkningen har blitt utført. Dette programmet er i utgangspunktet ikke beregnet til slik bruk, men det har likevel funksjoner som gjør dette mulig. I denne rapporten har programmets anvendelighet for denne typen bruk blitt vurdert.

Tre hovedmodeller har vært benyttet. Den første av disse var en meget enkel modell av et horisontalt rør som er senket ned i sjøen. Wire-kreftene ble vurdert, og det ble studert hvordan ulike input-parametere påvirket resultatene.

Input parameterne til den enkle modellen ble tatt videre til å simulere senkning av en undervanns-spool gjennom bølgesonen. Denne modellen bestod av en ”spool”, løftebjelke, fire løftestropper og en løftewire. Både flat sjø og regulære bølger ble simulert. Dette viste at slakk i løftewiren eller stroppene oppstod i 3 av 4 sjøtilstander. Videre ble elastiske utnyttelse av strukturen ble evaluert i henhold til API-RP-2A-WSD, som er implementert i USFOS. Resultatene fra dette studiet viste at den elastiske utnyttelsen av konstruksjonen økte når signifikant bølgehøyde økte. Men det kan imidlertid stilles spørsmål om hvor nøyaktig USFOS beregner kreftene i bølgesonen for de mest ekstreme tilfellene av regelmessige bølger.

Den siste og mest realistiske modellen som ble benyttet i denne avhandlingen var senkning av subsea spoolen i uregelmessige bølger. Disse bølger ble simulert i henhold til JONSWAP bølgespekteret. Ulike sjøtilstander ble modellert ved å endre verdien av signifikant bølgehøyde og topp-periode. I tillegg var den øverste enden av løftewiren koblet til kran på et fartøy. Fartøyets bevegelser ble definert av RAO funksjoner som var inkludert i programmets input filer. For alle de sjøtilstandene, ble den minste kraften i wiren og stroppene funnet. Dette resulterte i en oversikt over hvilke sjøtilstander som gav slakk i løftewiren eller stroppene. Trenden viste at når den signifikante bølgehøyden ble økt, ble minimums verdien av kreftene i

wiren og stroppene redusert. Fra arbeidet som ble utført ble det konkludert med at USFOS kan brukes til å modellere enkle marine løfteoperasjoner. Programmet beregner likevekts krefter i den øvre ende av wire-elementet riktig. Men dets bruk til dette formål er noe begrenset. Når demping innføres i systemet vil kraften i wire-elementet avta på grunn energi tap og dermed gi en feil i likevektsverdien. Videre krever den spesielle bjelkeformuleringen som brukes til å modellere wiren at en dynamisk analyse utføres. Dette vil føre til at det oppstår svingninger i systemet på grunn av igangsetting av tyngdekraften og egenvekt . Derfor bør den innledende fasen hvor disse oscillasjonene er til stede, neglisjeres når struktur responsen skal vurderes.

En av fordelene med USFOS når det gjelder denne typen bruk, er mulighetene programmet har til å modellere ikke-lineær oppførsel og beregne elastisk utnyttelse av strukturer. Det er imidlertid usikkerhet knyttet til det sistnevnte. Dette gjelder spesielt hvordan knekkfaktoren skal defineres mest realistisk. Derfor bør en være konservativ når denne skal velges.

# Contents

<b>List of Figures</b>	<b>xi</b>
<b>List of Tables</b>	<b>xiii</b>
<b>1 Introduction</b>	<b>1</b>
1.1 Scope . . . . .	1
1.2 Chapter overview . . . . .	2
<b>2 Lifting operations</b>	<b>5</b>
2.1 Forces acting during a lift . . . . .	7
2.1.1 Weight of lifted object and center of gravity . . . . .	7
2.1.2 Buoyancy forces . . . . .	8
2.1.3 Wave loads on structures . . . . .	9
2.1.4 Slamming . . . . .	11
2.1.5 Highest lifetime forces . . . . .	14
2.1.6 Snap loads in the lifting wire and slings . . . . .	14
2.1.7 Reducing forces due to limited lifting height . . . . .	16
2.2 Equation of motion of a structure lowered into the splash zone . . .	17
2.3 Modeling of marine operations . . . . .	18
<b>3 USFOS theory</b>	<b>19</b>
3.1 Build-up of the system . . . . .	19
3.2 Input files . . . . .	19
3.3 Dynamic analysis . . . . .	20
3.4 Hydrodynamics in USFOS . . . . .	20
3.4.1 Slamming . . . . .	21
3.4.2 Airy wave theory . . . . .	21
<b>4 Simple analyses in USFOS</b>	<b>23</b>
4.1 Model . . . . .	23
4.1.1 Modeling of the lifting wire . . . . .	25
4.1.2 Stiffness of the lifting wire . . . . .	26
4.1.3 Modeling of damping in the system . . . . .	27
4.1.4 Modeling of the waves . . . . .	27
4.2 Influence of time step size . . . . .	28
4.2.1 $dT=0.01s$ . . . . .	29
4.2.2 Comparison between different time steps . . . . .	30
4.2.3 Too large time step - $dT = 0.4$ . . . . .	31
4.3 Influence of damping on the system . . . . .	32

4.4	Constant lowering velocity . . . . .	33
4.5	Verification of model . . . . .	34
4.6	Results . . . . .	35
<b>5</b>	<b>Lowering of a subsea spool into flat sea and regular waves</b>	<b>37</b>
5.1	Model . . . . .	37
5.1.1	Modeling of coating . . . . .	39
5.1.2	Modeling of internal fluid and flooding . . . . .	40
5.1.3	Center of gravity . . . . .	40
5.1.4	Lifting wire . . . . .	41
5.1.5	Slings . . . . .	41
5.2	Lowering of model into flat sea . . . . .	43
5.2.1	Lowering of empty spool and empty spreader bar into flat sea	43
5.2.2	Lowering of filled spool and empty spreader bar into flat sea	44
5.2.3	Lowering of filled spool and flooded spreader bar into flat sea	44
5.2.4	Verification of equilibrium force in the wire . . . . .	46
5.3	Modeling of slack in USFOS . . . . .	48
5.4	Lowering of spool into regular waves . . . . .	49
5.4.1	Case 1 - H=3 , T=14.5, Dir=90, Phase=0 . . . . .	50
5.4.2	Case 2 - H=6 , T=12.5, Dir=90, Phase=0 . . . . .	50
5.4.3	Case 3 - H=8 , T=12.5, Dir=90, Phase=0 . . . . .	51
5.4.4	Case 4 - H=8 , T=8, Dir=90, Phase=0 . . . . .	51
5.4.5	Forces in wire and slings . . . . .	52
5.4.6	Code checking of structural response . . . . .	52
<b>6</b>	<b>Lowering of a subsea spool into irregular waves</b>	<b>55</b>
6.1	Model . . . . .	55
6.2	Cases of irregular waves . . . . .	56
6.3	Minimum forces in the wire and slings . . . . .	57
6.3.1	Discussion of results . . . . .	60
6.4	Maximum force in lifting wire - dynamic amplification factor . . . . .	61
<b>7</b>	<b>Conclusion</b>	<b>63</b>
<b>8</b>	<b>Suggestions for further work</b>	<b>65</b>
<b>9</b>	<b>Bibliography</b>	<b>67</b>

Appendices

Appendix A	Wave theory applicability	I
------------	---------------------------	---

Appendix B	RAO functions	III
Appendix C	Buckling factor for idealized boundary conditions	V
Appendix D	Discretization of spool model	VII





# List of Figures

2.1	Lifting of Suction Pile . . . . .	6
2.2	Buoyancy and weight forces on a lifting structure . . . . .	9
2.3	Slamming problem . . . . .	12
2.4	Water entry of circular cylinder . . . . .	13
2.5	Measures to avoid large stresses due to lifting slings . . . . .	16
3.1	USFOS input files . . . . .	20
3.2	Drag coefficient calculated in USFOS . . . . .	21
3.3	Wave definitions . . . . .	21
4.1	Lowering of a straight pipe . . . . .	24
4.2	Wire input . . . . .	26
4.3	Definition of wave heading . . . . .	28
4.4	Head file . . . . .	29
4.5	Wire forces and displacement for $dT = 0.01s$ . . . . .	30
4.6	Lowering velocity . . . . .	30
4.7	Force in the monitor element for different time step sizes . . . . .	31
4.8	Too large time step, $dT = 0.4s$ . Forces in lifting wire and global displacement . . . . .	32
4.9	Forces in the wire and monitor element for different damping . . . . .	33
4.10	Constant lowering velocity . . . . .	33
4.11	Velocity in global z direction of node 101 . . . . .	34
5.1	Spool model . . . . .	38
5.2	Displacement and force in monitor element for empty spool and empty spreader bar . . . . .	43
5.3	Displacement and force in monitor element for filled spool and empty spreader bar . . . . .	44
5.4	Parameters to define drain in the head file . . . . .	45
5.5	Displacement and force in monitor element for filled spool and flooded spreader bar . . . . .	45
5.6	Fill ration of spool and spreader bar . . . . .	46
5.7	Axial force in the wire and slings for case 1 . . . . .	50
5.8	Axial force in the wire and slings for case 2 . . . . .	50
5.9	Axial force in the wire and slings for case 3 . . . . .	51
5.10	Axial force in the wire and slings for case 4 . . . . .	51
5.11	Bending moment about local y axis . . . . .	54
6.1	Model description . . . . .	56
6.2	Minimum axial force in the lifting wire . . . . .	58

6.3	Minimum axial force in sling 600 . . . . .	58
6.4	Minimum axial force in sling 601 . . . . .	59
6.5	Minimum axial force in sling 602 . . . . .	59
6.6	Minimum axial force in sling 603 . . . . .	60
A.1	Wave theory applicability . . . . .	I
B.1	RAO for surge, sway and heave . . . . .	III
B.2	RAO for roll, pitch and yaw . . . . .	IV
C.1	Buckling factors for idealized boundary conditions . . . . .	V
D.1	Discretization of the spool . . . . .	VII
D.2	Discretization of the spreader bar . . . . .	VIII

# List of Tables

4.1	Pipe Data . . . . .	25
4.2	Wire Data . . . . .	27
4.3	Calculation of equilibrium force . . . . .	35
5.1	Spool data . . . . .	39
5.2	Center of gravity . . . . .	40
5.3	Wire Data . . . . .	41
5.4	Sling Data . . . . .	42
5.5	Equilibrium force in the hoisting wire. Comparison between calculated values and USFOS values . . . . .	47
5.6	Cases of different wave parameters . . . . .	49
5.7	Elastic utilization according to API WSD . . . . .	53
6.1	Cases of iregular waves with 45 degree heading . . . . .	57
6.2	Dynamic amplification factors for the different seastates . . . . .	62



## Abbreviations

<b>CB:</b>	center of buoyancy
<b>CF:</b>	center of force resultant, F
<b>CG:</b>	center of gravity
<b>RAO:</b>	response amplitude operator



## Symbols

$a$ :	body acceleration [ $m/s^2$ ]
$A$ :	cross section area of cylinder [ $m^2$ ]
$A_{33}$ :	added mass in z direction [kg]
$A_p$ :	horizontal projected area of an object [ $m^2$ ]
$a_r$ :	relative acceleration between body and fluid particles [ $m/s^2$ ]
$B_{33}^{(1)}$ :	linear damping coefficient in z direction [ $kg/s$ ]
$B_{33}^{(2)}$ :	quadratic damping coefficient in z direction [ $kg/m$ ]
$C_A$ :	added mass coefficient [-]
$C_M$ :	mass coefficient [-]
$C_D$ :	drag coefficient [-]
$C_s$ :	slamming coefficient [-]
$c(t)$ :	wetted radius of body used in slamming calculations [m]
$D$ :	cylinder diameter [m]
$DAF_{max}$ :	maximum dynamic amplification factor for a time series [-]
$dF(t)$ :	wave load per unit length [ $N/m$ ]
$dF_s$ :	slamming force per unit length [ $N/m$ ]
$\Delta L$ :	incremental change in length [m]
$D_o$ :	outer diameter [m]
$E$ :	modulus of elasticity [Pa]
$\eta$ :	displacement of lifted object in z direction [m]
$\dot{\eta}$ :	velocity of lifted object in z direction [ $m/s$ ]
$\ddot{\eta}$ :	acceleration of lifted object in z direction [ $m/s^2$ ]
$F_b$ :	buoyancy force [N]

$F_c$ :	steady force due to current [ $N$ ]
$F_d$ :	drag force [ $N$ ]
$F_e$ :	water exit force [ $N$ ]
$F_I$ :	inertia force [ $N$ ]
$F_{max}$ :	maximum dynamic force in a time series [ $N$ ]
$F_s$ :	slamming force [ $N$ ]
$F_{snap}$ :	snap load [ $N$ ]
$F_{static}$ :	static equilibrium force in the wire [ $N$ ]
$F_w$ :	wave excitation force [ $N$ ]
$F_{wd}$ :	wave damping force [ $N$ ]
$F_{wire}$ :	force in the lifting wire [ $N$ ]
$g$ :	gravity acceleration ( $9.81 \text{ m/s}^2$ )
$H$ :	wave height [ $m$ ]
$h$ :	distance from the bottom of a horizontal cylinder to the sea surface [ $m$ ]
$H_s$ :	significant wave height [ $m$ ]
$j$ :	subscript that indicates the element number
$K$ :	stiffness [ $N/m$ ]
$k_{wire}$ :	wire stiffness [ $N/m$ ]
$L$ :	length [ $L$ ]
$\lambda$ :	wave length [ $m$ ]
$L_i$ :	initial length of the lifting wire [ $m$ ]
$m$ :	mass of lifted object [ $kg$ ]
$m_j$ :	mass of element $j$ [ $kg$ ]
$N$ :	total number of structural parts [-]



$R$ :	cylinder radius [ $m$ ]
$r$ :	displacement amplitude of member [ $m$ ]
$\rho$ :	water density [ $kg/m^3$ ]
$\rho_i$ :	inner fluid density [ $kg/m^3$ ]
$\rho_s$ :	material density [ $Pa$ ]
$\sigma_u$ :	ultimate tensile strength [ $Pa$ ]
$\sigma_y$ :	yield stress [ $Pa$ ]
$T$ :	wave period [ $s$ ]
$t_c$ :	coating thickness [ $m$ ]
$\Theta$ :	wave heading [ $deg$ ]
$T_p$ :	spectral peak period [ $s$ ]
$t_w$ :	wall thickness [ $m$ ]
$v$ :	fluid particle velocity (waves and/or current) [ $m/s$ ]
$V(t)$ :	displaced volume at time $t$ [ $m^3$ ]
$v_3$ :	fluid particle velocity in $z$ direction [ $m/s$ ]
$\dot{v}_3$ :	fluid particle acceleration in $z$ direction [ $m/s^2$ ]
$\ddot{v}$ :	fluid particle acceleration [ $m/s^2$ ]
$v_r$ :	relative velocity between body and fluid particles [ $m/s$ ]
$V_{rel}$ :	relative velocity between load and crane tip [ $m/s$ ]
$W_0$ :	weight of object in air [ $N$ ]
$\bar{x}$ :	$x$ coordinate of CG [ $m$ ]
$\bar{x}_j$ :	$x$ coordinate of element $j$ 's CG [ $m$ ]
$\bar{y}$ :	$y$ coordinate of CG [ $m$ ]
$\bar{z}$ :	$z$ coordinate of CG [ $m$ ]
$\dot{\zeta}$ :	vertical velocity of the sea surface [ $m/s$ ]



# 1 Introduction

The offshore oil and gas exploitations often requires that subsea equipment is installed on the seabed. Such equipment can be manifolds, pumping systems and suction piles. Many operations that are done today require calm weather conditions, and are therefore limited to the summer period.

Prior to a lifting operation it is necessary to define the limiting seastates accurately. This is in order to ensure that the operation is performed safely. There are several methods for doing this, some more conservative than others. DNV (2011) gives a Recommended Practice for Modelling and Analysis of Marine Operations. It also gives a simplified method for estimation of characteristic forces acting on objects that are lifted through the splash zone. The method can in general be characterized as a conservative approach, especially for larger structures. In this case, numerical analysis using commercial software such as MACSI and SIMO is necessary (Sarkar and Gudmestad; 2010). The success of such analyses depends on accurate definitions of important parameters, such as wire stiffness and hydrodynamic coefficients Gordon et al. (2014)

## 1.1 Scope

This thesis will investigate the applicability for using USFOS to simulate marine lifting operations. The computer program is not initially intended for such use, but it has features that still make this possible. Further on, the structural response of a subsea spool model will be considered. USFOS will also be used for code checking of the structures response histories.

The initial scope of work says that the results from USFOS should be compared with alternative software such as SIMO. However, during the thesis work it was learned that it was time consuming to find the best way to simulate operations in USFOS. Therefore it was decided, in collaboration with the supervisor, that the items regarding the alternative software was to be neglected (items 2, 5 and 7). Additionally the focus is put more on how USFOS can be used to model marine lifting operations rather than code checking of structural response histories. Lastly, dynamic buckling will not be covered by the thesis.

Thus the scope that is covered in this thesis takes the following form:

- Review of various subsea installations and equipment that will be installed by

lift operations. Discuss the expected load conditions that will be encountered and potential failure modes that must be controlled. From this overview, select the scenarios that will be investigated by simulation. It is suggested that focus be placed on installations and equipment where Morrison forces and slamming forces will be important.

- Familiarize with USFOS for modeling the lifting behavior by establishing a very simple, idealized model. The starting point is the given finite element model.
- Establish the finite element model in USFOS for the cases selected for analysis. The model will include the installation/equipment, the wires and the crane. The lifting vessel/barge may be modelled as a two-node element, with one node in the centre of gravity. The vessel motions may be simulated on the basis of transfer functions for wave induced displacement or wave forces for various incoming wave angles.
- Establish finite element models for simulations with alternative software.
- Perform simulation of the lifting operations for the selected scenarios. This may comprise both lift off, through the splash zone and landing on sea floor. The environmental conditions shall be varied. Extreme load cases shall be sought. Of particular interest may be intense, short duration load pulses caused by wave slamming or contact forces during landing. Evaluate the risk of yielding or buckling according to API RP2A WSD by utility tool for code checking of structural response. To facilitate large parametric variations it should be considered to automatize these simulations by using scripts.
- On the basis of the experience obtained in pt. 5 discuss the the appropriateness of the tools for simulations of marine operations. Discuss challenges that may need to be resolved. Conclusions and recommendations for further work

## 1.2 Chapter overview

In chapter 2 theory regarding lifting operations will be presented. This will include different types of operations, forces present in a lifting operation and common failure modes for lifting operations.

Chapter 3 will describe the most relevant theory behind the computer program USFOS. This is to give the reader a better understanding of what is done in chapter 4 and 5.

In chapter 4, a simple pipe model will be considered. The focus will be put on how to use the input parameters and how USFOS can be applied to simulate operations.

Chapter 5 will continue to simulate lifting operations. The model of a subsea spool will be considered. This will be lowered both into flat sea and regular waves. Different sea states will be modeled, and the structural response will be discussed. In these simulations the top of the lifting wire is not moving.

Chapter 6 will involve the model of the same spool as before. In this chapter, the top of the lifting wire is connected to the crane of a vessel model. The vessel moves according to given response amplitude operator (RAO) functions. Several cases of irregular waves are considered, and the structural response is looked in to.

Chapter 7 and 8 is conclusion and recommendations for further work, respectively.



## 2 Lifting operations

As the offshore industry operates on deeper seas, subsea technology become more and more important. This again means that marine lifting operations of subsea equipment are very common. A normal procedure is to transport the subsea structures from land to the offshore installation site, using a transportation barge. When arriving on the installation site, the subsea structure is transferred to the rig or the installation vessel (Bai and Bai; 2012). An example of the lifting of a suction pile into the sea is given in figure 2.1.

Nielsen (2007) gives the following examples of such operations:

- Crane assisted installation of jacket structures.
- Installation of deck modules
- Installation of subsea equipment such as templates, spool pieces, manifolds, protection structures etc.

Crane operations are often divided into two categories, based on the lifted weight compared to the lifting vessel. These are called light and heavy lifts. Nielsen (2007) explains these as follows:

*Light lifts* is the term used for lifts where the load is very small compared to the vessel. This means that the load has a small influence on the vessel motion. In this case the weight of the lifted object is less than 1-2% of the vessels displacement. For lifts in this category, heave compensation can often be used to reduce vertical motions of the load .

The second of the two categories is *heavy lifts*. This category cover lifts where the load influences the vessel motion. Due to this, dynamic coupling between the lifted object and the vessel must be considered in analyses. Oppose to the case of light lifts, the load is in these cases more than 1-2% of the vessels displacements (more than 1000 tons). For lifts in this category, heave compensation is not possible.

A typical subsea lift can be divided into 4 main phases (DNV; 2011):

- Lift off from deck and maneuvering the lifted object clear of the transportation vessel
- Lowering through the wave zone

- Further lowering down to the sea bed
- Positioning and landing on the sea bottom

DNV (2011) recommends that all of these phases are evaluated before a lifting operation is performed.

In this thesis, the focus will be on the second phase, lowering through the splash zone. To simulate this phase of the lift accurately can be very challenging. This is due to all of the forces that need to be considered. These include hydrodynamic forces, time varying buoyancy, motion of the lifting vessel and snap loads (Gordon et al.; 2014). It is critical to get a good estimation of the wave loads during this phase, because they often determine the limiting sea states of an operation (Araujo et al.; 2012)



Figure 2.1: Lifting of Suction Pile (Parimi and Qian; 2008)



## 2.1 Forces acting during a lift

When a structure is lowered into the water both the structure and the hoisting system will be exposed to various forces. (DNV; 2011) recommends that the following forces are taken accounted for when looking at the response of an object:

- $F_{wire}$  = Force in the lifting wire
- $W_0$  = Weight of object in air
- $F_b$  = Buoyancy force
- $F_c$  = Steady force due to current
- $F_I$  = Inertia force
- $F_{wd}$  = Wave damping force
- $F_d$  = Drag force
- $F_w$  = Wave excitation force
- $F_s$  = Slamming force
- $F_e$  = Water exit force

The proceeding sections will describe these forces further.

### 2.1.1 Weight of lifted object and center of gravity

The weight of the lifted object in air can be calculated according to equation 2.1.

$$W_0 = mg \tag{2.1}$$

where

- $m$  = mass of the lifted object [kg]
- $g$  = gravity acceleration [ $m/s^2$ ]

When planning a lifting operation it is critical to know the location of the center of gravity, CG, of the lifted object. This is due to the arrangement of slings and lifting wire during the lift. Design codes usually accounts for the uncertainty in the CG calculations. This, however, depends on which code that is applied (Alv er; 2012).

The center of gravity can be calculated by using momentum calculations. Consider a structure that can be divided into  $N$  elements. The  $x$  coordinate of the structures CG can be found in the following way:

$$\bar{x} = \frac{\sum_{j=1}^N m_j \bar{x}_j}{\sum_{j=1}^N m_j} \quad (2.2)$$

where

- $N$  = number of elements [-]
- $j$  = element number (1, 2, ...,  $N$ )
- $\bar{x}_j$  =  $x$  coordinate of element  $j$ 's CG
- $m_j$  = mass of element  $j$  [kg]

The  $y$  and  $z$  coordinates of the CG can be found in the same way by replacing  $\bar{x}$  in equation 2.2 with  $\bar{y}$  and  $\bar{z}$ , respectively.

### 2.1.2 Buoyancy forces

The buoyancy forces acting on a submerged object is calculated as the weight of the water displaced by the body. The force resultant from the buoyancy will act in the center of the submerged volume. This is not necessarily the same as the center of gravity. The resulting moment between the two forces, can therefore lead to rotations of the submerged body. Equation 2.3 shows how the buoyancy force can be calculated:

$$F_b = \rho g V(t) \quad (2.3)$$

where

- $\rho$  = water density [ $kg/m^3$ ]
- $V(t)$  = displaced volume of water at time  $t$  [ $m^3$ ]

Figure 2.2 shows an example of how the buoyancy and gravity force act on a lifted structure. It can be observed that the offset of the center of buoyancy (CB) and center of gravity (CG) leads to a heel angle of the object. The resulting force center (CF) is also indicated.

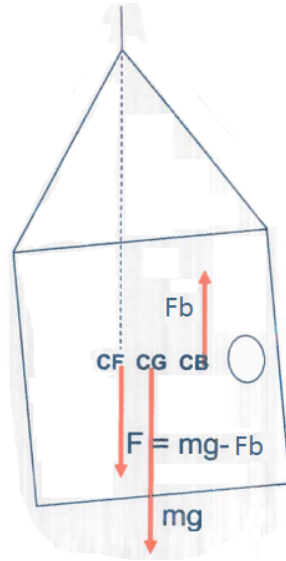


Figure 2.2: Buoyancy and weight forces on a lifting structure(Sandvik; 2007)

Equation 2.4 shows how the force center, CF, can be found. If the vertical added mass is not in line with the resulting force F, the structure will be subjected to tilting oscillations (Sandvik; 2007).

$$CF = \frac{F_b * CB - mg * CG}{mg - F_b} \quad (2.4)$$

where

$$m = \text{mass of the lifted object [kg]}$$

The location of the center of buoyancy for a submerged structure, is found by calculating the center of submerged volume. This is done in a similar way as for the COG, replacing the mass with volume in eq. 2.2.

### 2.1.3 Wave loads on structures

To estimate the drag and inertia forces on a cylindrical structure, a Morison formulation can be used. This is valid for small volume structures that has dimensions, D, smaller than the typical wave lengths  $\lambda$ , of waves exciting the structure. Faltinsen (1990) present Morison's equation in the following way:

$$dF(t) = \rho AC_M \dot{v} + \frac{\rho}{2} C_D D v |v| \quad (2.5)$$

where

$$C_M = 1 + C_A \quad (2.6)$$

where

$$\begin{aligned} dF(t) &= \text{wave load per unit length [N/m]} \\ C_M &= \text{mass coefficient [-]} \\ C_A &= \text{added mass coefficient [-]} \\ C_D &= \text{drag coefficient [-]} \\ v &= \text{fluid particle velocity [m/s]} \\ \dot{v} &= \text{fluid particle acceleration [m/s}^2\text{]} \\ D &= \text{cylinder diameter [m]} \\ A &= \text{cross section area of the cylinder [m}^2\text{]} \end{aligned}$$

Equation 2.5 can normally be used when the structure and waves satisfy the condition,  $\lambda > 5D$ . The equation has two parts. *The first* is proportional to the fluid acceleration,  $\dot{v}$ , and is called the mass force. This can again be divided into the Froude-Krilof force and the diffraction force. *The second part* of eq. 2.5 is proportional to the square of the fluid velocity,  $v$ , and is called the drag force .

The coefficients  $C_D$  and  $C_M$  are drag and mass coefficients respectively.  $C_A$  is the added mass coefficient. In reality, these have to be determined empirically and depend on many different parameters. From potential theory, it can be shown that for  $C_M = 2$  for cylindrical structures (Faltinsen; 1990).

If a moving structure is studied, which will be the case in this thesis, equation 2.5 can be expressed in terms of relative velocity as (DNV; 2011):

$$dF(t) = \rho A a + C_A A a_r + \frac{1}{2} \rho C_D D v_r |v_r| \quad (2.7)$$

where:

$$\begin{aligned} a &= \text{body acceleration [m/s}^2\text{]} \\ a_r &= \text{relative acceleration between body and fluid particles [m/s}^2\text{]} \\ v_r &= \text{relative velocity between body and fluid particles [m/s]} \end{aligned}$$

Equation 2.7 is often termed the relative velocity formulation. When using this formulation DNV (2011) states that additional hydrodynamic damping should normally not be included. Further on they describe equation 2.7 to be applicable for the drag force if the following is satisfied:

$$r/D > 1 \quad (2.8)$$

In equation (2.8)  $r$  is the displacement amplitude of the member and  $D$  is the member diameter.

### 2.1.4 Slamming

When a structure is lowered into water it is exposed to several loads. One of these loads is called slamming, and is defined as impulse loads with high pressure peaks between a body and a liquid during impact. These loads can be high and potentially damaging to the structure. From a structural point of view slamming is a problem both locally and for the global elastic behavior.

The magnitude of the slamming load and its features are determined by factors such as relative velocity between body and the water and the shape of the body. Dynamic and kinematic conditions at the time of impact are also affecting the slamming.

An example of slamming is when the ship bottom hits the water surface with a high velocity. Another is when breaking waves hit the columns of an offshore platform. This can cause fatigue damage on the structure (Faltinsen; 1990).

For marine lifting operations slamming loads occur when structures are lifted through the splash zone. This is defined as one of the critical stages of such an operation. The slamming loads can cause damage to the structure that is lowered. Additionally the loads can contribute to a decreased tension in the lifting wire and slings. If this decrease is too large, slack in the slings and the lifting can occur, followed by large snap loads. This can be very critical to the hoisting system (described in section 2.1.6).

There are several ways to calculate the slamming loads on a structure. For calculating the slamming loads on a blunt body, normal practice is to consider the boundary value problem shown in figure 2.3.

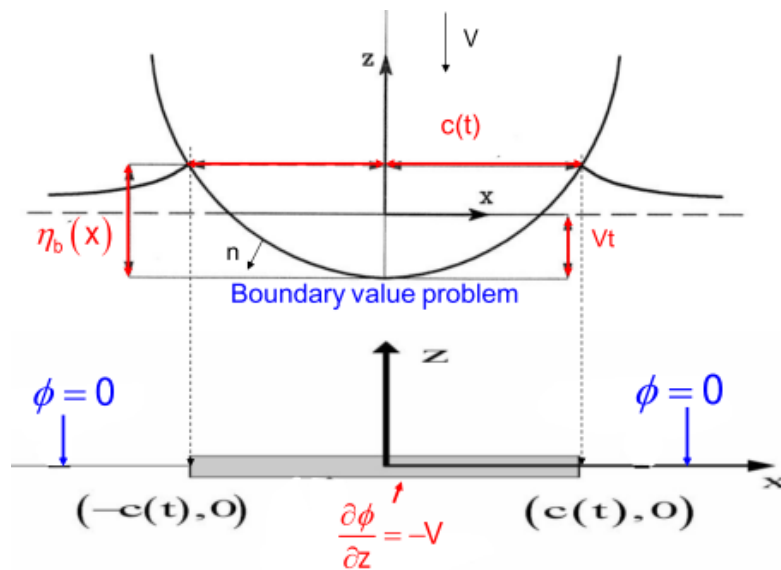


Figure 2.3: Slamming problem (Faltinsen; 1990)

Figure 2.3 shows the blunt body a small time instant  $t$  after impact. At this time the draft of the body is  $Vt$  and its wet surface is between  $-c(t) \leq x \leq c(t)$ .

To evaluate the slamming loads on a structure, it is necessary to know the value of  $c(t)$ . There are two basic methods that can be used to find this analytically (Greco; 2012). These are Von Karman's and Wagner's approach. One of the main differences between these two methods is whether or not they account for the water rise up during slamming. Von Karman neglects this effect when estimating  $c(t)$ , whereas Wagner's method takes this effect into account. This means that the predicted wetted surface is larger according to Wagner's approach than according to Von Karman.

Faltinsen (1990) presents the results from numerical simulations performed by Campbell and Weynberg (1980). They did experiments to find the slamming loads on cylinders. Compared to the two approaches described earlier, Campbell and Weynberg (1980) give a smaller value than Wagner's approach and a larger value than Von Karman's approach. The reason for the difference between experimental and the theoretical values is that the present theory does not predict the wetted surface in the right way (Faltinsen; 1990).

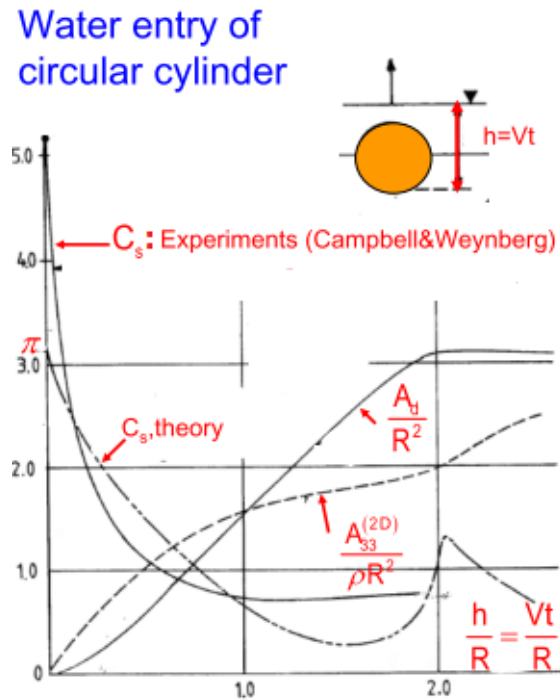


Figure 2.4: Water entry of circular cylinder (Greco; 2012)

Figure 2.4 show the experimental value of the slamming coefficient,  $C_s$ , from Campbell and Weynberg (1980). This is also the curve that is implemented in the computer program USFOS to calculate the slamming loads. Faltinsen (1990) presents this curve by the following equation:

$$C_s = \frac{5.15}{1 + 8.5 \frac{h}{R}} + 0.275 \frac{h}{R} \quad (2.9)$$

where:

- $h$  = distance from the bottom of a horizontal cylinder to the sea surface [m]
- $R$  = cylinder radius [m]

When the slamming coefficient  $C_s$  is calculated, the corresponding slamming force,  $F_s$ , can be found by using the following relationship:

$$C_s = \frac{dF_s}{\frac{\rho}{2} 2RV^2} \quad (2.10)$$

The force  $dF_s$  in equation 2.10 is the slamming force per unit length of the cylinder. The total force on a cylinder can be found by integrating  $dF_s$  over the length  $L$ .

### **2.1.5 Highest lifetime forces**

The highest lifetime forces of different subsea structures often occurs during installation. Sandvik (2007) describes the highest lifetime forces of subsea structures to be:

General:

- Snap loads at lift-off or after slack
- Impact after uncontrolled pendulum motion
- Local loads from wave impact

Further Sandvik (2007) gives examples of different structures and the highest lifetime forces for these:

Templates and trawl protection:

- Wave forces in the splash zone

Suction anchor:

- Wave forces in the splash zone
- Soil penetration forces

Spool pieces:

- Forces during lift in air
- Wave forces near the surface

Steel pipe:

- Bending stresses over stinger or at the sea bed, and during tie in.
- Wave forces near the surface

### **2.1.6 Snap loads in the lifting wire and slings**

The lifting wire and slings that are used to lift offshore structures do not support compressive loads. They only have capacity in tension, which means that there is a possibility that the lifting wires or slings go slack during a lift. This can happen when the loads acting against the direction of the lift become larger than the weight of the lifted object. I.e when the structure is lowered into the splash zone.



When the slack wire/slings goes back into tension, a sudden shock load will occur in the wire. This load is often called a snap or snatch load. Its magnitude can be many times greater than the dynamic equilibrium forces in a steady state response (Thurston et al.; 2014). The load can lead to rupture of the wire or slings, or failure of the shackle between these. It can also be damaging to the crane or the lifted object.

Equation 2.11 shows how the snap load,  $F_{snap}$ , can be calculated (Sandvik; 2007).

$$F_{snap} = F_{static} + V_{rel} \sqrt{k_{wire}(M + A_{33})} \quad (2.11)$$

where:

- $k_{wire}$  = wire stiffness [ $N/m$ ]
- $m$  = mass of the lifted object [ $kg$ ]
- $A_{33}$  = added mass in z direction of the lifted object [ $kg$ ]
- $V_{rel}$  = relative velocity between the load and the crane tip [ $m/s$ ]
- $F_{static}$  = static equilibrium force in the wire [ $N$ ]

Notice that when the lifted object is hanging in the wire in air,  $F_{stat}$  is equal to the weight of the lifted object,  $Mg$  (if the self-weight of the wire is neglected).

Because of the large magnitude of the snap load, it can be very critical for the lifting operation if slack in the lifting wire or slings occurs. Therefore the simplified method by DNV (2011), recommends that the tension force in the lifting slings does not become less than 10% of the static submerged weight of the lifted structure. If however slack can't be avoided, DNV (2011) recommends a conservative approach to estimate the snap load. This approach is to assume that the structure is falling with a constant velocity, and is stopped by the hoisting system.

It can be observed that regulations or recommended practices regarding lifting operations have weaknesses when it comes to snap load estimation and they often over predict the tension in the lifting wire. This again leads to less weight being lifted (Thiagarajan et al.; 2001).

Many studies have been done on snap loads and how to avoid these. Gordon et al. (2014) simulated the lowering of a suction pile using the computer program SIMO (see Figure 2.1). They studied how parameters such as lowering velocity, wave period and significant wave height, affect the probability of slack in the hoisting wire. It is shown that the probability of slack increases as the significant wave height increases. This is also the case for lowering velocity. The opposite is true

for the period,  $T_p$ . An increase in this leads to a decreased probability of slack wire.

### 2.1.7 Reducing forces due to limited lifting height

If the angle of the lifting slings are too small relative to the horizontal plane, large stresses can occur in the structure. In order to avoid this it is common practice to use a spreader beam, lifting frame or compression bars to connect the slings with the lifted structure. Figure 2.5 shows some examples of how this arranged in practice.

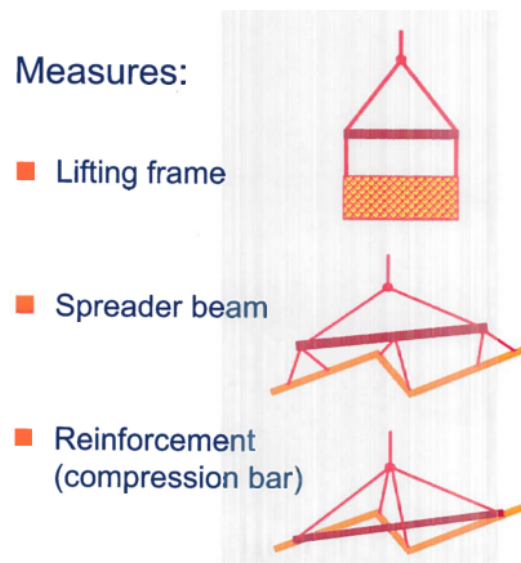


Figure 2.5: Measures to avoid large stresses due to lifting slings (Sandvik; 2007)

## 2.2 Equation of motion of a structure lowered into the splash zone

If a structure with dimensions much smaller than the wavelength of the incoming waves is considered, the vertical motion  $\eta(t)$  can be described in terms of the forces acting on the structure (DNV; 2011):

$$(M + A_{33})\ddot{\eta} = B_{33}^{(1)} + B_{33}^{(2)}(v_3 - \dot{\eta})|(v_3 - \dot{\eta})| + (\rho V + A_{33})\dot{v}_3 + \frac{\rho}{2}C_s A_p (\dot{\zeta} - \dot{\eta})^2 + \rho g V(t) - Mg + F_{wire} \quad (2.12)$$

where

$B_{33}^{(1)}$	=	linear damping coefficient in z direction [kg/s]
$B_{33}^{(2)}$	=	quadratic damping coefficient in z direction [kg/m]
$v_3$	=	water particle velocity in z direction [m/s]
$\dot{v}_3$	=	water particle acceleration in z direction [m/s <sup>2</sup> ]
$\eta$	=	displacement of lifted object in z direction [m]
$\dot{\eta}$	=	velocity of lifted object in z direction [m/s]
$\ddot{\eta}$	=	acceleration of lifted object in z direction [m/s <sup>2</sup> ]
$F_{wire}$	=	force in the lifting wire [N]
$A_p$	=	horizontal projected area of an object [m <sup>2</sup> ]
$\dot{\zeta}$	=	vertical velocity of sea surface [m/s]
$V(t)$	=	displaced volume at time t [m <sup>3</sup> ]

The equation above expresses the vertical motion of a lifted structure in terms of buoyancy, wave excitation, inertia, slamming and drag damping forces. (DNV; 2011). In this equation the drag damping force is divided into two parts. The first part is proportional to the relative velocity ( $v_3 - \dot{\eta}$ ), and has a linear damping coefficient  $B_{33}^{(1)}$ . The second part is proportional to the square of the relative velocity. This force term depends on quadratic damping coefficient  $B_{33}^{(2)}$  (DNV; 2011).

The force in the wire can be defined as (DNV; 2011):

$$F_{wire} = Mg - \rho g V(t) + k_{wire}(z_{ct} - \eta) \quad (2.13)$$

In equation 2.13, it can be seen how the forces and motions in the system affect the force in the lifting wire. The parameter  $z_{ct}$  is the vertical motion of the crane tip, while  $\eta$  is the motion of the lifted object. Thus the difference  $z_{ct} - \eta$  describes the stretching/shortening of the lifting wire. Multiplied with the wire stiffness,  $k_{wire}$ , the stiffness force in the wire is found. When lowering the structure into the water, the wire length will increase. This means that the stiffness of the wire,  $EA/L$ , will

decrease. In other words, the vertical stiffness of the system will decrease as the structure is lowered into the sea.

## 2.3 Modeling of marine operations

In order to determine which sea states that are critical for a certain operation it is common to use standards created by companies such as DNV. They have developed a recommended practice for modeling and analysis of marine operations (DNV; 2011). This also gives a simplified method for calculation of the hydrodynamic loads. The method is a conservative approach that is good for initial design purposes.

An alternative to this is to perform numerical analyses using software such as SIMO . Such analyses can be very time consuming and require hundreds of different simulations to define the limits for an operation (Gordon et al.; 2014).

## 3 USFOS theory

This chapter will describe the relevant theory behind the computer program USFOS. The purpose of this is to get a better understanding of what is done later on in the report.

The analyses performed in this thesis work is done by the computer program USFOS. This program is intentionally made for doing non-linear analysis of marine structures. Examples of such usage is ultimate strength analysis and progressive collapse analysis of space frame structures . The programs basic idea is to use only one finite element per physical element in the structure. This is the same that is done in linear, elastic analysis (SINTEF Group; 2001).

The program is not initially intended for being used to model marine operations. But it has, however, several features that still make this possible. The work done in this thesis will test how USFOS can be used for this sort of application.

### 3.1 Build-up of the system

The USFOS system has three main program modules (SINTEF Group; 2001):

- The USFOS analysis module does all of the numerical calculations. It generates at least two files of analysis data, depending on type of analysis. The analysis-print file (.out) is a text file where general results is printed. The second file is the analysis-data file (.raf). This is a binary file that contains structure data as well as result data from the analysis.
- The POSTFOS module extracts data from the USFOS binary result database. It generates text files of selected analysis results.
- XACT is the general user interface (GUI) of the program. This reads the analysis data file through POSTFOS and gives a three dimensional visualization of the model. Results from the analysis can be presented as color plots and graphs. It can also show animations of dynamic analyses.

### 3.2 Input files

To run analyses in USFOS the user have to define two input files. These files are a head file and a structure file (fig.3.1). The structure file contains structural and

load data. In the head file, control parameters that define the analysis is written (SINTEF Group; 2001). In this work the head file also contains hydrodynamic parameters. When these two files are defined, the analysis can be carried out.

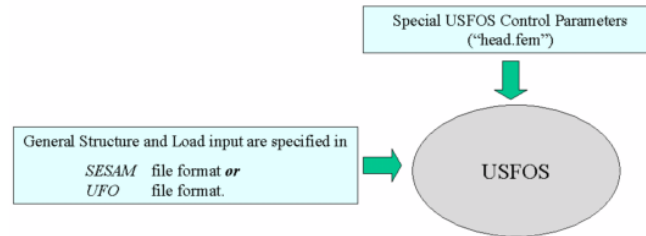


Figure 3.1: USFOS input files (SINTEF Group; 2001)

### 3.3 Dynamic analysis

USFOS can do dynamic analysis for given load-time history. There are two options for defining the mass of the structural element. The first is consistent mass and the second is lumped mass. In this work the lumped mass option will be used. This means that the mass matrix is diagonal. The rotational masses are scaled by a factor called "rotmass".

The damping of the system can be given as Rayleigh damping. This type of damping has two terms. One that is proportional to the mass matrix, and another that is proportional to the stiffness matrix. These two terms damp out lower and higher modes of vibration, respectively (SINTEF Group; 2001).

The numerical integration in USFOS is based on the HHT- $\alpha$  method. To get numerical stability during the integration, the time step length must be defined in the right way. It must be smaller than a given fraction of the fundamental eigenperiod of the system (SINTEF Group; 2001).

### 3.4 Hydrodynamics in USFOS

When modeling marine operations, the hydrodynamic input in USFOS becomes important. The following will give a short description of the relevant input that will be used in the analyses. The material is taken from Usfos As (2010).

### 3.4.1 Slamming

The program calculates the slamming loads on cylinders according to the Campbell and Weynberg experimental values (eq: 2.9). This calculated the slamming coefficient from the relative submergence of the body. USFOS updates the drag coefficient according to this. When the cylinder is fully submerged ( $h/r = 2$ ) the user defined drag coefficient is used (Holmås; 2010).

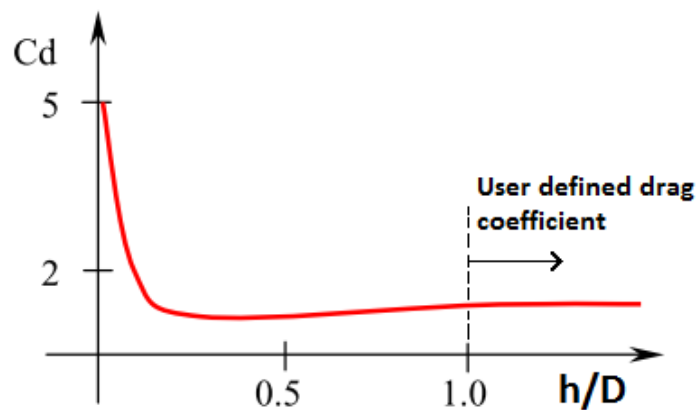


Figure 3.2: Drag coefficient calculated in USFOS (Holmås; 2010)

### 3.4.2 Airy wave theory

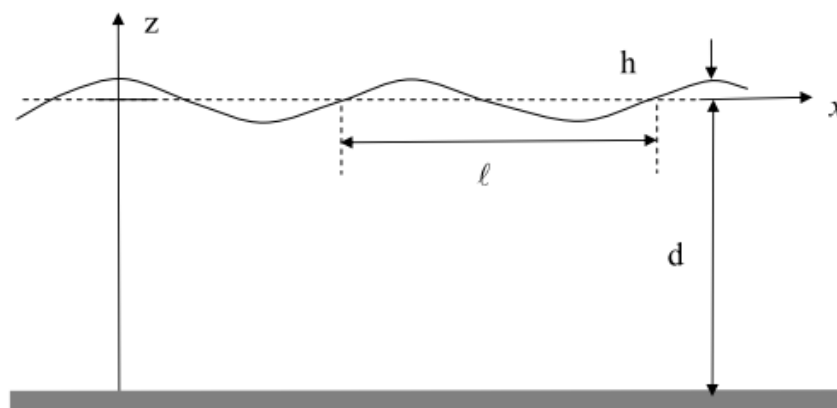


Figure 3.3: Wave definitions (Usfos As; 2010)

If deep water is assumed,  $\frac{d}{\lambda} > 0.5$ , the wave potential from Airy theory is given by:

$$\phi = \frac{gh}{\omega} e^{-kz} \cos(\omega t - k \cos \theta x - k \sin \theta y) \quad (3.1)$$



# 4 Simple analyses in USFOS

In order to get a better understanding of how USFOS can be used to model marine operations, a simple model considered. This consist of a 45m horizontal steel pipe that is lowered through the splash zone with two lifting wires (see Figure 4.1).

Several cases using the same model are studied. This gives a better insight on how different input parameters affect the results.

The following cases are studied :

- Influence of time step size - what time step is necessary to achieve good results?  
What will be the effect of too large steps?
- Influence of damping. What is the effect of including/excluding damping from the model.
- Effect of constant lowering velocity.

## 4.1 Model

The model consist of a straight pipe with a total length of 45 meters. The data of the model is given in table 4.1.

Two wires attached to each side of the pipe, is used to lower the structure into the water. Both the nodes where the wires are connected to the pipe are also subjected to a point-load. (see Figure 4.1). The wires are modeled as two tension-springs, with an initial spring coefficient corresponding to the initial elastic stiffness of the wires. The top of both of these wire elements are connected to two additional pipe elements. These will be referred to as "monitor" elements and are used to check if USFOS calculates the forces in the wire elements correctly. The top nodes of the monitor elements are defined as fixed in all degrees of freedom.

As the pipe is submerged it will not be flooded with sea water.

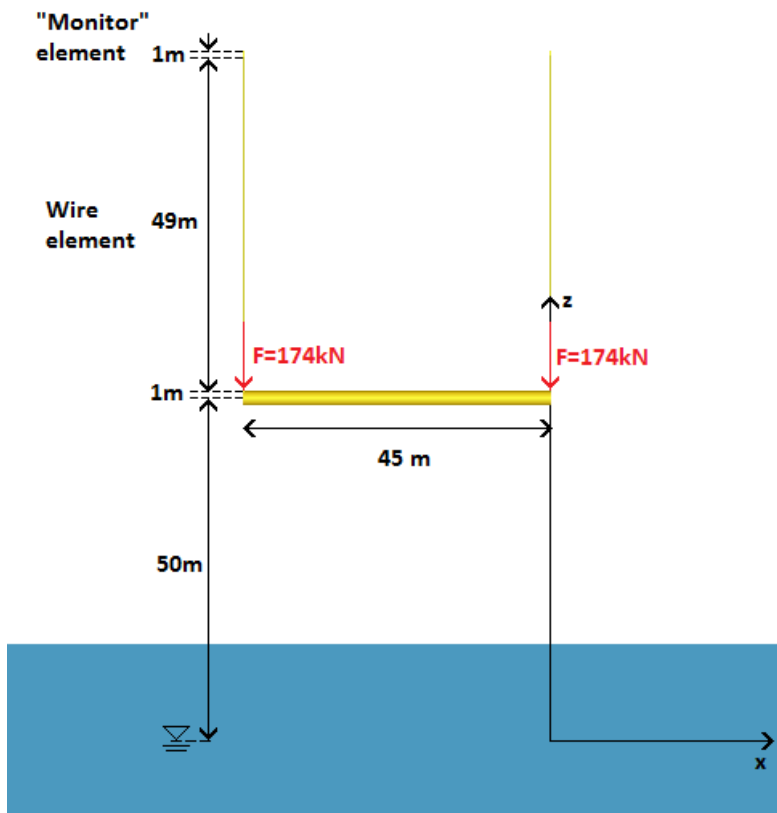


Figure 4.1: Lowering of a straight pipe

Table 4.1: Pipe Data

	Parameter	Value	Unit
Outer diameter	$D_o$	2	[m]
Wall thickness	$t_w$	0.1	[m]
Length	$L$	45	[m]
Cross section area	$A$	0.6	[m <sup>2</sup> ]
Modulus of elasticity	$E$	2.10E+11	[Pa]
Yield stress	$\sigma_y$	5.00E+10	[Pa]
Material density	$\rho_s$	7850	[kg/m <sup>3</sup> ]
Water density	$\rho$	1024	[kg/m <sup>3</sup> ]
Gravity acceleration	$g$	9.81	[m/s <sup>2</sup> ]

#### 4.1.1 Modeling of the lifting wire

Lowering of the structure is modeled by increasing the "tension free" length of the two wire-elements. The length is increased by a factor of 2 in the time interval 10 s to 100 s. This increase follows a S-curve to avoid too sudden accelerations in the wires when the lowering starts and stops (see Figure 4.5b). If, on the other hand, a constant rate of length increase is used the whole way, large oscillations will be present initially. This is due to the sudden acceleration in the start of the lowering (see Figure 4.10a).

The wire elements are modeled by using a special beam formulation available in USFOS. This is done in the following way; A material of the type "TensSpri" is defined in the structural file. This material is again assigned a time history ID. The two wire elements are then defined to have this special material type (see Figure 4.2b).

In the "head" file the time history assigned to the material is defined (see Figure 4.2a). Here an initial time,  $T_1$ , and an end time,  $T_2$ , is defined. The special beam element elongates with a factor, "fac", from time  $T_1$  to  $T_2$ . This elongation follows an S-curve that is of order "pow". The S-curve can be defined to have an order of 1, 2 or 3. I.e a power of 1 will just be a linear elongation (constant velocity).

It is the "tension free" length of the element that is increased. This means that if the size of the time step is sufficiently small, there will not be introduced any restoring force,  $EA/dL$ , due to the elongation of the wire elements. A further description of the input parameters is given in Usfos As (2014).

```

'
      Elem ID   np1   np2  material   geom   lcoor   ecc1   ecc2
BEAM      2000    102   2000    3000     3
BEAM      2001    101   2001    3000     3
'
      matno   Type   Typ    K           Gap  Rho  Hist
Material 3000  TensS   1     1.69E7     0.0  0.0  1001
'

```

(a) Wire input in the structure file

```

'
      Typ    T1  T2  Fac  Pow
TimeHist 1001  S_Curv  10  100  2   3
'

BeamType 5    Mat 3000
'

```

(b) Wire input in the head file

Figure 4.2: Wire input

### 4.1.2 Stiffness of the lifting wire

The stiffness of the lifting wire is defined in the structure input file (see Figure 4.2a). From this figure we can see that the stiffness is set to be  $1.69E7N/m$ . This is found in the following way:

$$k_{wire} = \frac{EA}{L} \quad (4.1)$$

where

$$A = \frac{\pi}{4}D^2 \quad (4.2)$$

Table 4.2 gives geometric data and the initial stiffness for the lifting wires. As the wire length,  $L$ , is increased, the corresponding stiffness,  $K$ , will decrease (according to eq. 4.1). The stiffness of the wires is updated for each time-step.

Table 4.2: Wire Data

Wire data	Parameter	Value	Unit
Diameter	$D$	0.1	[ $m$ ]
Wall thickness	$t_w$	0.04	[ $m$ ]
Elastic modulus	$E$	1.10E+11	[ $Pa$ ]
Cross section area	$A$	7.54E-03	[ $m^2$ ]
Initial length	$L_i$	49	[ $m$ ]
Stiffness	$k_{wire}$	1.69E+03	[ $N/m$ ]

### 4.1.3 Modeling of damping in the system

To include damping to the whole system, rayleigh damping is used. In addition two damping elements are included, one parallel to each of the wires.

It is hard to determine the damping of the system correctly. It can therefore be questioned how realistic the used damping values are. However, in a real system, there will always be a certain energy loss due to friction etc.

In addition to the structural damping of the system, hydrodynamic damping due to drag is also included.

### 4.1.4 Modeling of the waves

The waves are modeled by using the Airy wave formulation used in USFOS as described in chapter ???. For this model the same waves are used in all the different cases. The wave height,  $H$ , is set to be  $1m$  and the period,  $T$ , is set to be equal to 14 seconds. Wave heading,  $\Theta$ , is set to be 90 degrees (see Figure 4.3).

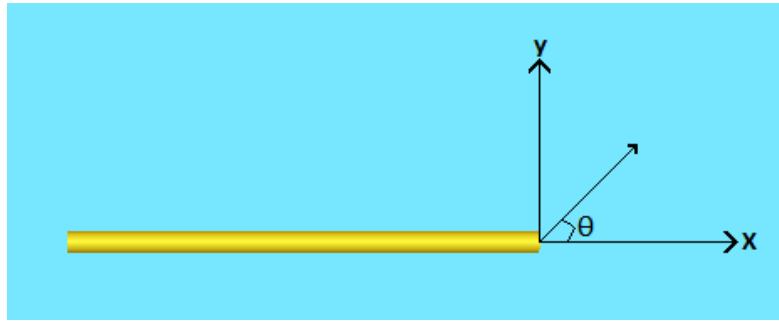


Figure 4.3: Definition of wave heading

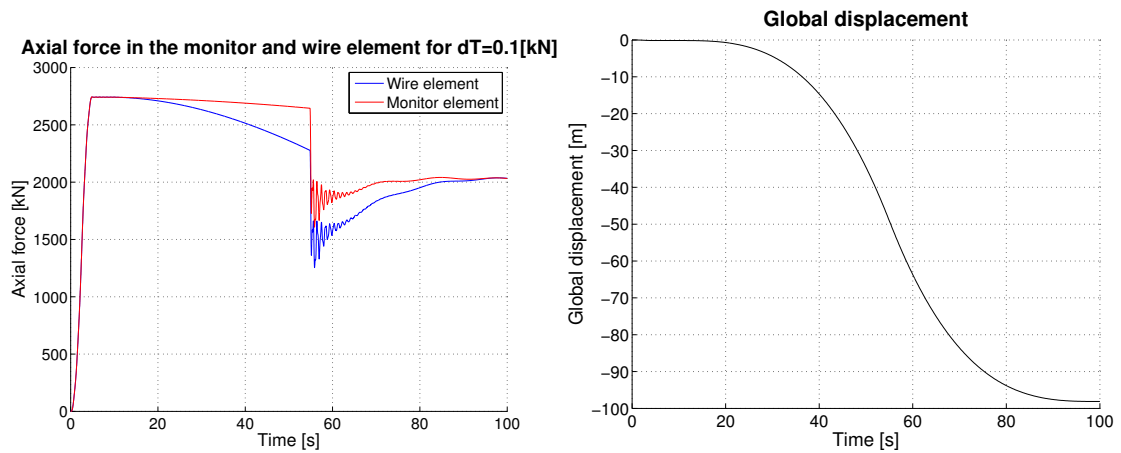
## 4.2 Influence of time step size

Several analyses have been run using different time step  $\Delta L$ . This is done in order to get a better understanding of which time step values that are sufficient to use to obtain a good result. If the incremental change of the wire length,  $\Delta L$ , is too large, the force in the wire will go to zero. The following cases of time step size will be presented in this section:

- $dT = 0.001s$
- $dT = 0.01s$
- $dT = 0.1s$
- $dT = 0.4s$

An example of the head file where the time step is defined is given in figure 4.4.





(a) Axial force in wire and monitor element (b) Global displacement of the structure.

Figure 4.5: Wire forces and displacement for  $dT = 0.01s$

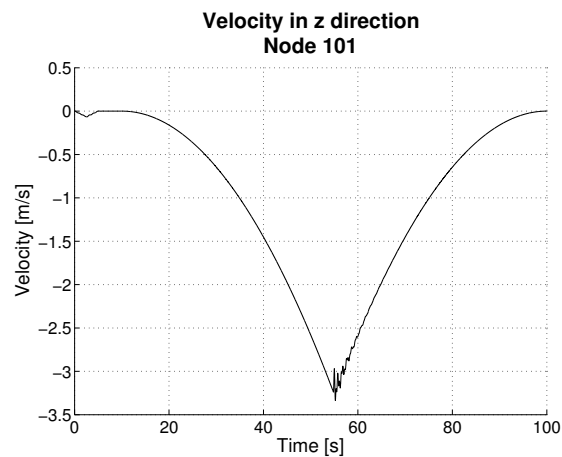


Figure 4.6: Lowering velocity

### 4.2.2 Comparison between different time steps

Figure 4.7 shows the force history of the monitor element for three different timesteps. As the plots show, the forces are nearly equal in all of the cases. This indicates that  $dT = 0.01s$  is sufficiently large time step for this analysis.



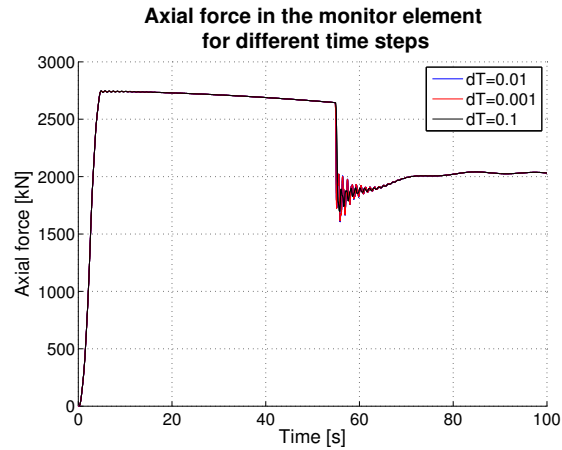
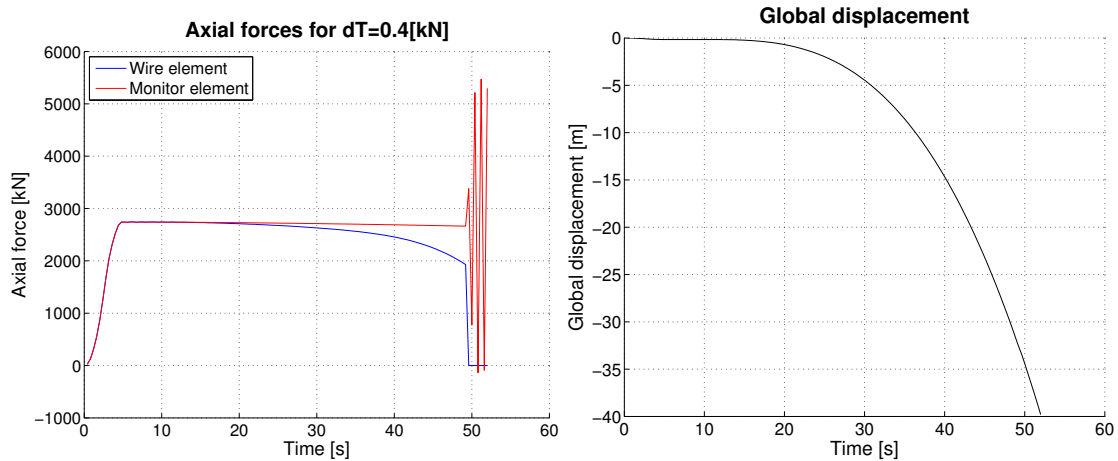


Figure 4.7: Force in the monitor element for different time step sizes

### 4.2.3 Too large time step - $dT = 0.4$

If the timestep is too large, the incremental change of the wire length will be too large. Thus  $\Delta L = \Delta T \dot{\eta}$  will become too large. When this happens, the force in the wire will go to zero. An example of this is when the time step,  $\Delta T$ , is set to be equal to 0.4 s. This will result in the wire force shown in figure 4.8. From the figures it can be observed that the analyses fails around  $t = 52s$ . The force in the wire elements goes to zero at  $t = 48s$ . This is due to too large incremental change of the length.

The global displacement starts to follow an scurve, but stops when the analysis fail.



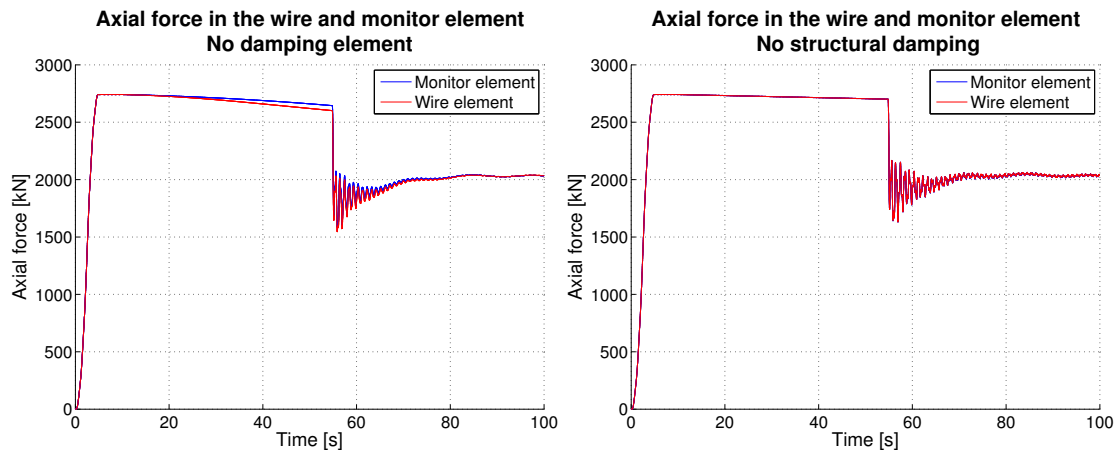
(a) Axial force in wire and monitor element (b) Global displacement of the structure.

Figure 4.8: Too large time step - Forces in lifting wire and global displacement

### 4.3 Influence of damping on the system

Figure 4.9a shows the forces in the wire and monitor elements when the spring damping elements are turned off. It can be observed that in this case, the force in the wire is much closer to the force in the monitor element. However, the energy loss in the wire element is still lower than that of the monitor elements from  $t = 5s$  to  $t = 54s$ . This is because the rayleigh damping has a bigger effect on the elongated wire element than it has on the monitor element. This is again due to the relative velocity between the top and bottom node of the wire element when this is elongated.

Figure 4.9b shows the forces when no structural damping is introduced. The only damping in this model is hydrodynamic damping. For this case, the force in the wire and the monitor elements are the same. However it can be observed that there is a small decrease in the force from the lowering start until the structure reaches the water ( $5s \leq t \leq 54s$ ). This decrease is about  $40kN$  ( $2741kN - 2701kN$ ). One of the reasons for the decrease can be the fact that lowering velocity is not constant but increasing. Thus there will be inertia forces due to the acceleration of the lowered structure. This will reduce the tension force in the wire.



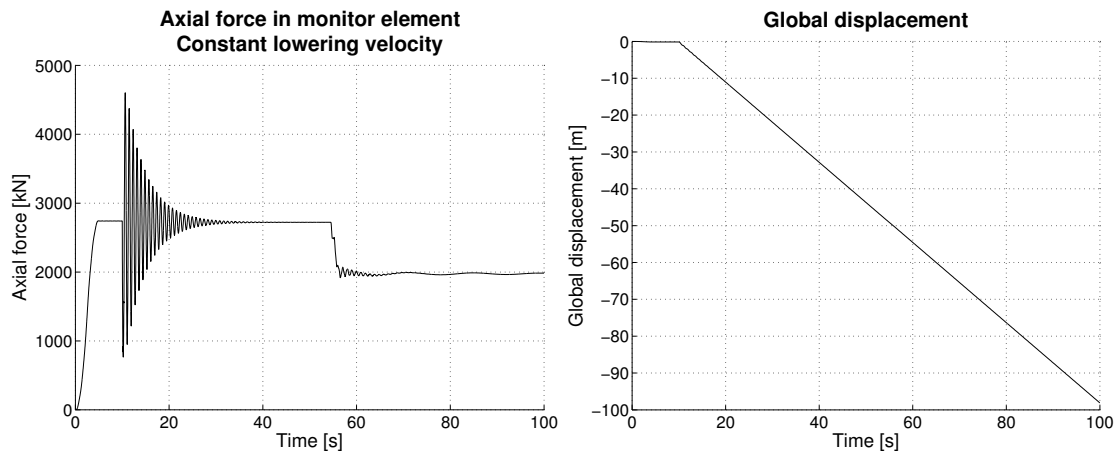
(a) No damping elements, only Rayleigh damping

(b) No structural damping

Figure 4.9: Forces in the wire and monitor element for different damping

## 4.4 Constant lowering velocity

In the previous cases the lowering followed an scurve. Thus the lowering velocity was not constant. If however a constant velocity was used from the beginning the force in the monitor element would be as shown in figure 4.10a (elongation is defined as an s-curve with order 1). The vertical displacement of the structure will thus be linear (see Figure 4.10b).



(a) Axial force in wire and monitor element (b) Global displacement of the structure.

Figure 4.10: Constant lowering velocity

The vertical velocity of the pipe is plotted in figure 4.11. It can be seen that the same initial oscillations as for the forces, occurs for the velocity. After these are damped out, the velocity stabilizes on about  $-1.2m/s$ . The velocity at water impact (at  $t = 55s$ ) is lower than for the case where the velocity was not constant. Thus the slamming forces are expected to be lower for this case. From this it is again expected that the wire force is higher in the splash zone for the constant velocity case. If the plots for the two cases are compared it can be observed that the wire force in the splash zone is higher for the case where the velocity is lower (see Figures 4.10a and 4.5a).

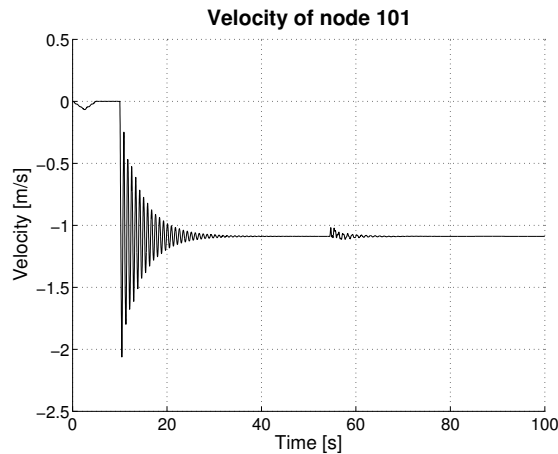


Figure 4.11: Velocity in global z direction of node 101

## 4.5 Verification of model

To verify that USFOS calculates the correct equilibrium force in the wire elements, calculations have been done for both in air and when submerged. The results of these calculations are shown in table 4.3. The USFOS results are for the two "monitor" elements at the top of the wires. Because the wires are modeled with very low density ( $\rho = 10kg/m^3$ ), the weight of the wires are neglected in this calculation.

From the table it can be seen that the calculated values are relatively close to the USFOS values. The USFOS values are about 0.36% higher than the calculated wires when the force is in air. For the submerged case the calculated values are 1.5% higher than the values from USFOS. This gives a good indication on that USFOS calculates the equilibrium forces in the lifting wire in the right way.

Table 4.3: Calculation of equilibrium force

	Calculations	USFOS	Diff	Unit
Pipe mass	2.11E+05			[kg]
Pipe weight	2.07E+06			[N]
Total force in nodes*	3.41E+06			[N]
Volume displacement	1.41E+02			[m <sup>3</sup> ]
Total gravitational force	5.48E+06			[N]
Total buoyancy force***	1.42E+06			[N]
Force in each wire**	2.74E+06	2.75E+06	1.00E4	[N]
Force in each wire***	2.03E+06	2.00E+06	-3.00E4	[N]

\* The sum of the two additional forces in the wire-pipe connections

\*\* In air

\*\*\* Fully submerged

## 4.6 Results

From this chapter it have been shown how USFOS can be used to model lowering a horizontal straight pipe. Calculations show that the program calculates the correct equilibrium values for the wire forces in both air and when the pipe is fully submerged. The program also seem to capture the most important hydrodynamic effects in a simplified way. It is however questionable how good it is to model the lifting wire in the way that USFOS does. Especially if the length of the wire becomes too large. In this case the analysis will become more sensitive to time step size

In the next chapter, a subsea spool will be modeled. The modeling done in this chapter will be taken further and effects on the structure as well as the wires will be considered.



# 5 Lowering of a subsea spool into flat sea and regular waves

In the following chapter the lowering of a subsea spool into sea will be modeled. The study on how USFOS can be used to simulate marine lifting operations will be taken further. Because USFOS is not usually used for modeling such lifting operations, many variations of input have been tested in an attempt to model the operation in a good and realistic way. The main analysis that were run during this iterative process, will be shown and discussed in this chapter. The structural response of the spool will also be investigated.

## 5.1 Model

The operation that is simulated in this chapter is the lowering of a subsea spool into the sea. This is one of the first phases in the installation. A subsea spool is a hard pipe that is typically used to connect manifold systems to wells on the sea bed. Subsea spools often has a bended shape. Therefore it is normal to use a "spreader bar" during installation to avoid high stresses due to the lifting slings (see Figure 2.5). The spreader bar is to be removed from the spool after the spool is installed on the seabed. This will not be considered in this work.

The model consist of a subsea spool, a spreader bar, 4 slings and the hoisting wire. Figure 5.1 shows the model in three planes. From this it can be seen that two slings are connected to the spreader bar and two are conected to the spool. The other ends of these four slings are connected to the lifting wire in a point above the spool. On the top end, the lifting wire is connected to a "monitor" element, as in chapter 4. The boundary conditions of this element are the same as previously which was fixed in all 6 degrees of freedom.

Different cases of flooding and filling of the model have been modeled. This will be explained further in section 5.2

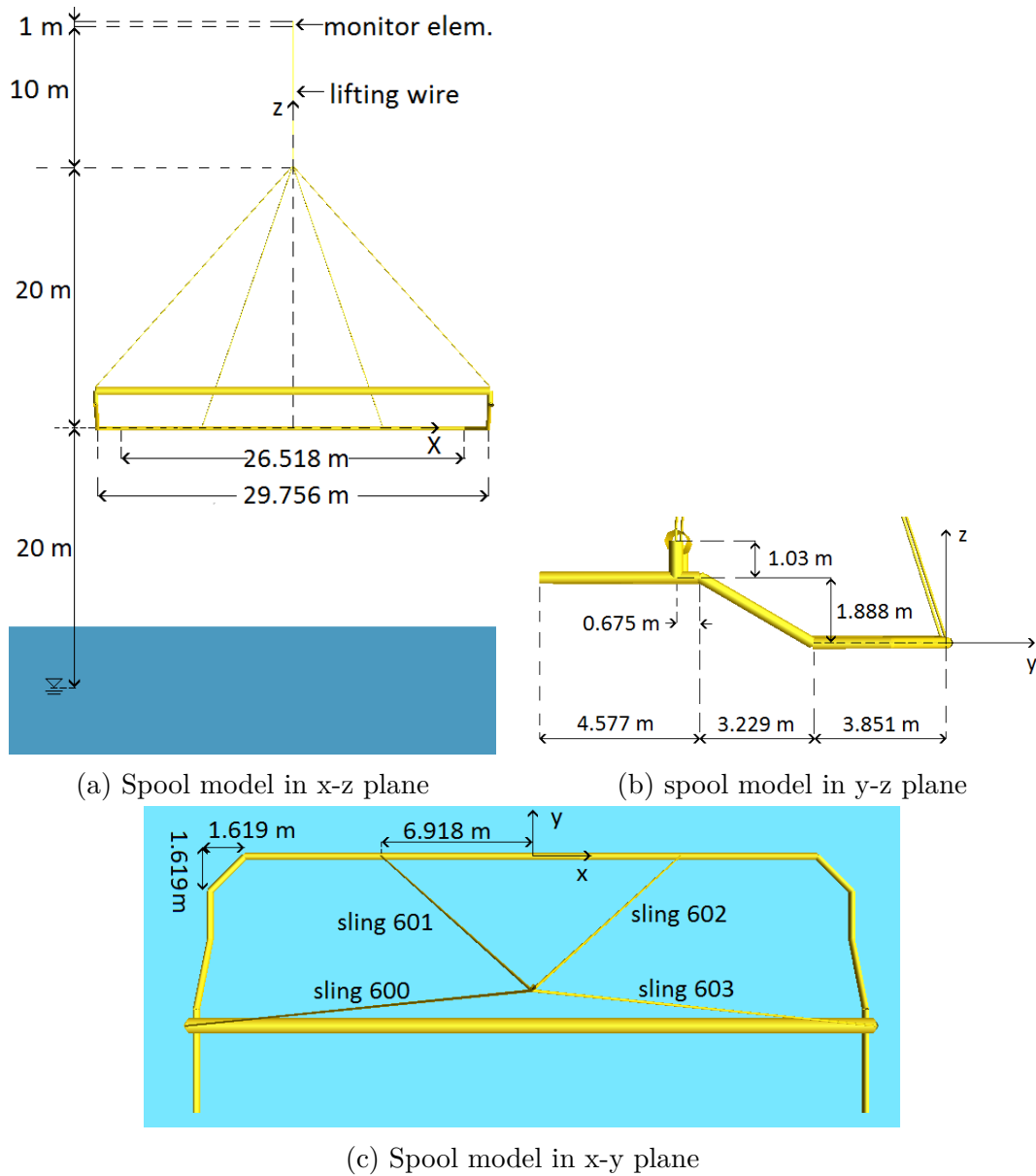


Figure 5.1: Spool model. The spool is symmetric about the y-axis



Table 5.1: Spool data

<b>Spool</b>	Parameter	Value	Unit
Outer steel diameter	$D_o$	0.3239	[m]
Wall thickness	$t_w$	0.0127	[m]
Coating thickness	$t_c$	0.003	[m]
Cross section area*	$A_s$	0.0124	[m <sup>2</sup> ]
Total cross section area**	$A$	0.0155	[m <sup>2</sup> ]
Modulus of elasticity	$E$	210	[GPa]
Yield stress	$\sigma_y$	550	[MPa]
Material density	$\rho_s$	7850	[kg/m <sup>3</sup> ]
Inner fluid density	$\rho_i$	1100	[kg/m <sup>3</sup> ]
<b>Spreader bar</b>			
Modulus of elasticity	$E$	210	[GPa]
Yield stress	$\sigma_y$	355	[MPa]
Material density	$\rho_s$	7850	[kg/m <sup>3</sup> ]
<i>Main part</i>			
Outer diameter	$D_o$	0.6604	[m]
Wall thickness	$t_w$	0.0254	[m]
Cross section area	$A$	0.0506	[m <sup>2</sup> ]
Length	$L$	30	[m]
<i>Connections</i>			
Outer diameter	$D_o$	0.4064	[m]
Wall thickness	$t_w$	0.0159	[m]
Cross section area	$A$	0.0195	[m <sup>2</sup> ]
Length	$L$	1.33	[m]
<b>Environmental data</b>			
Water density	$\rho$	1024	[kg/m <sup>3</sup> ]
Gravity acceleration	$g$	9.81	[m/s <sup>2</sup> ]

\* Area of cross section without coating

\*\* Area of cross section with coating

### 5.1.1 Modeling of coating

In this work, it is assumed that the coating of the spool does not contribute significantly to the structural strength. The coating is assumed to only increase the hydrodynamic diameter of the spool. Thus the coating can be modeled as ma-

rine growth in USFOS, using the MARGROWTH parameter in the head file. In addition to this the BuDiam parameter is used to include the coating also in the buoyancy calculations.

By doing this, USFOS takes the coating into account when calculating all the hydrodynamic loads on the spool.

### 5.1.2 Modeling of internal fluid and flooding

Subsea spools are often filled with an internal fluid during the installation. This fluid is typically MEG (Ethylene glycol) based gel. Its purpose is to protect the spool from corrosion. (Søfteland; 1990). In this thesis work the density of the gel is set to be  $1100 \text{ kg/m}^3$ .

The spreader bar is empty in air, but will be flooded with sea water as it is submerged.

Three different cases of internal fluid and flooding have been studied. These will be explained in more detail in section 5.2.

### 5.1.3 Center of gravity

In all the cases that are run in this chapter, the top of the slings and top of the lifting wire are placed over the spools CG in air. The COG of the spool is found for both the empty and filled condition. It is calculated according to equation 2.2. Table 5.2 show the main results from this calculation. The table shows that the x value of the CG is zero in all the cases. This is because the spool is modeled to be symmetric about the y axis.

Table 5.2: Center of gravity. Coordinates are according to the global coordinate system

Case	x	y	z	Unit
Empty in air	0.00	-6.318	2.202	[m]
Filled spool in air	0.00	-5.648	1.879	[m]
Submerged*	0.00	-6.284	2.189	[m]

\* Spreader bar flooded and spool filled

### 5.1.4 Lifting wire

The lifting wire has the properties shown in table 5.3. Its geometry is a pipe section with a large wall thickness relative to the radius. The wire is modeled as a spring element that increases its length according to a given time history. This is done by using the same special beam formulation that was used in chapter 4.

Table 5.3: Wire Data

Wire data	Parameter	Value	Unit
Outer diameter	$D$	0.08	[ $m$ ]
Wall thickness	$t_w$	0.03	[ $m$ ]
Elastic modulus	$E$	8.80E10	[ $Pa$ ]
Cross section area	$A$	4.71E-03	[ $m^2$ ]
Initial length	$L$	10	[ $m$ ]
Stiffness	$k_{wire}$	4.15E7	[ $N/m$ ]

### 5.1.5 Slings

The structure is connected to the hoisting wire with 4 slings. Two that are connected to the spreader bar (600 and 603) and two connected to the spool (601 and 602). Each of the two pairs are placed symmetrical about the y-axis (see Figure 5.1c).

The slings are modeled as beam elements. Thus they have capacity in tension as well as compression. They can also have bending moments. In reality the slings only have capacity in tension and will go slack if the tension force go to zero. This means that compression in the sling elements will correspond to slack slings. This should be checked in the results.

Further on, the sling elements used in USFOS have capacity in bending. In reality there would be no bending moment present in the slings. To reduce the bending moments in the sling elements, the ends of each element are modeled as hinges in the local ry and rz direction. Thus no bending moment in these DOF's will be transferred from neighboring elements.

The slings have the properties shown in table 5.4. Their lengths are different for the filled and empty conditions. This is due to different position of the COG

of the model and thus different position of the top point of the slings (see Table 5.2). The stiffness of the slings are calculated according to equation 4.1

Table 5.4: Slings Data

Slings data	Parameter	Value	Unit
<i>Properties</i>			
Outer diameter	$D$	0.08	[m]
Wall thickness	$t_w$	0.03	[m]
Elastic modulus	$E$	880E8	[MPa]
Cross section area	$A$	0.0047	[m <sup>2</sup> ]
<b>Empty spool</b>			
<i>Slings 600 and 601</i>			
Length	$L$	22.45	[m]
Stiffness	$K$	1.85E7	[N/m]
<i>Slings 602 and 603</i>			
Length	$L$	21.94	[m]
Stiffness	$K$	1.89E7	[N/m]
<b>Filled spool</b>			
<i>Slings 600 and 601</i>			
Length	$L$	22.5	[m]
Stiffness	$K$	1.84E7	[N/m]
<i>Slings 602 and 603</i>			
Length	$L$	21.76	[m]
Stiffness	$K$	1.91E7	[N/m]

## 5.2 Lowering of model into flat sea

The first that was done was to model the lowering of the spool and spreader bar into calm water. Several different variations in the input file was tested in order to find a good way to do this. In this section the following three cases will be described:

- Lowering of empty spool and spreader bar into flat sea
- Lowering of filled spool and empty spreader bar into flat sea
- Lowering of filled spool and flooded spreader bar into flat sea

For each case plots of the global displacement and wire force are shown (see Figures 5.2, 5.3 and 5.5) The last case will then be taken further when different environmental conditions will be considered (see Section 5.4).

### 5.2.1 Lowering of empty spool and empty spreader bar into flat sea

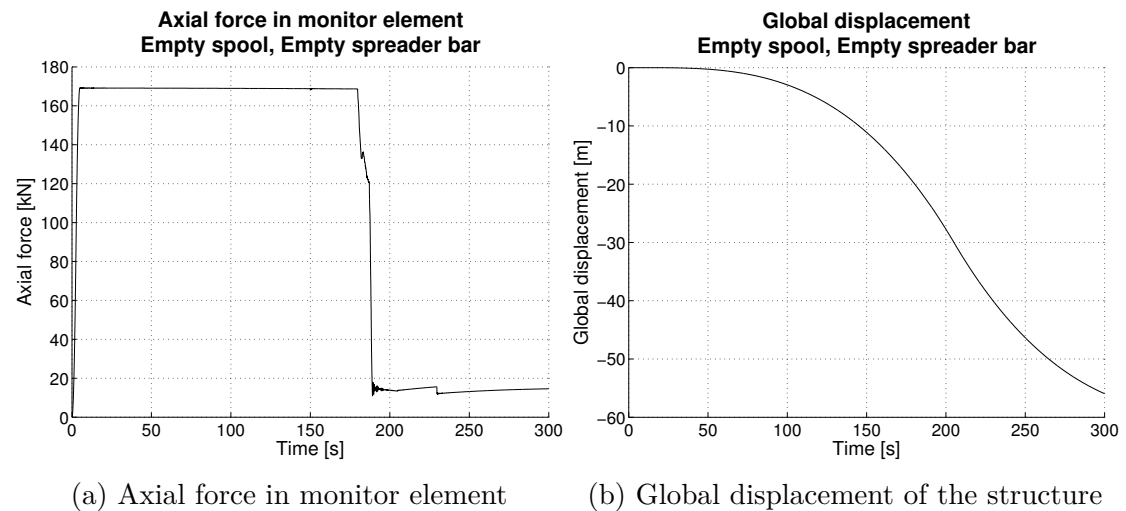


Figure 5.2: Displacement and force in monitor element for empty spool and empty spreader bar

## 5.2.2 Lowering of filled spool and empty spreader bar into flat sea

The next step is to let the spool be filled with an internal fluid at the start of the simulation. In this analysis the fluid is defined to have a density of  $1100 \text{ kg/m}^3$ . As described in section 5.1.2, the spool is filled with an internal fluid during the installation. This is modeled by using the INTFLUID parameter in the head file (citepUSFOS2014). The parameter is connected to a time history that defines the spool to be filled with this fluid from the time 0 to 5s. This means that the spool is completely filled before the lowering starts at  $t = 10\text{s}$ .

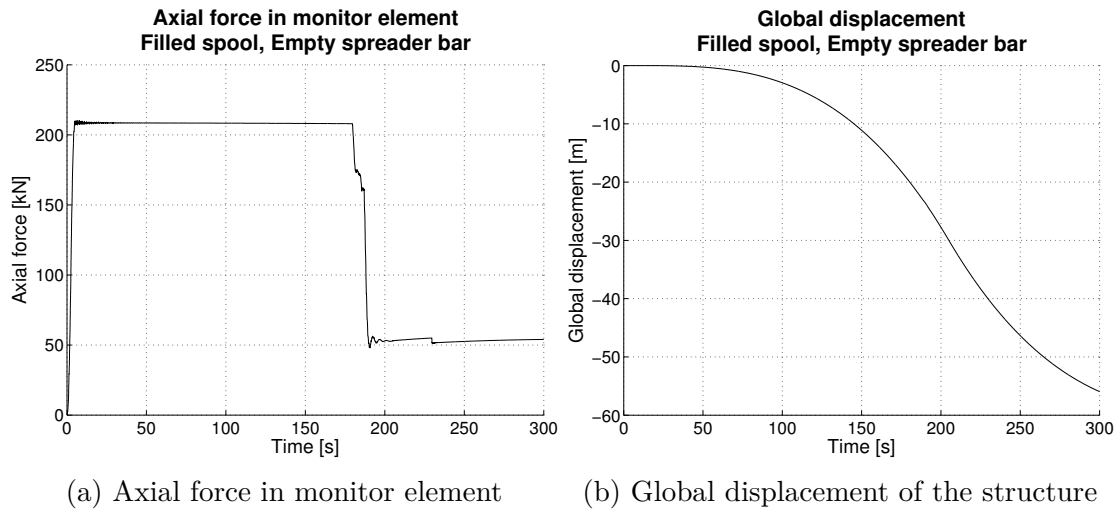


Figure 5.3: Displacement and force in monitor element for filled spool and empty spreader bar

## 5.2.3 Lowering of filled spool and flooded spreader bar into flat sea

The final configuration of the model is that the spool is filled with fluid initially (as in Section 5.2.2) and the spreader bar is filled with seawater as it is submerged. By designing the spreader bar so that it lets sea water in, the buoyancy forces of the structure will decrease as the spreader is filled. In this way the tension force in the wire and slings will be larger than if the spreader bar was empty. This again leads to a reduced probability of slack in the wire.

For this purpose the "Drained" parameter is used together with the "INTFLUID" parameter in USFOS (Usfos As; 2014). Figure 5.4 shows the three lines that is necessary in the head file to model the flooding in such a way. When using this

technique, the user must define the drain time. That is the time it takes from the body is submerged until it is filled with seawater. The drain time is set to be 30 seconds for this model.

```

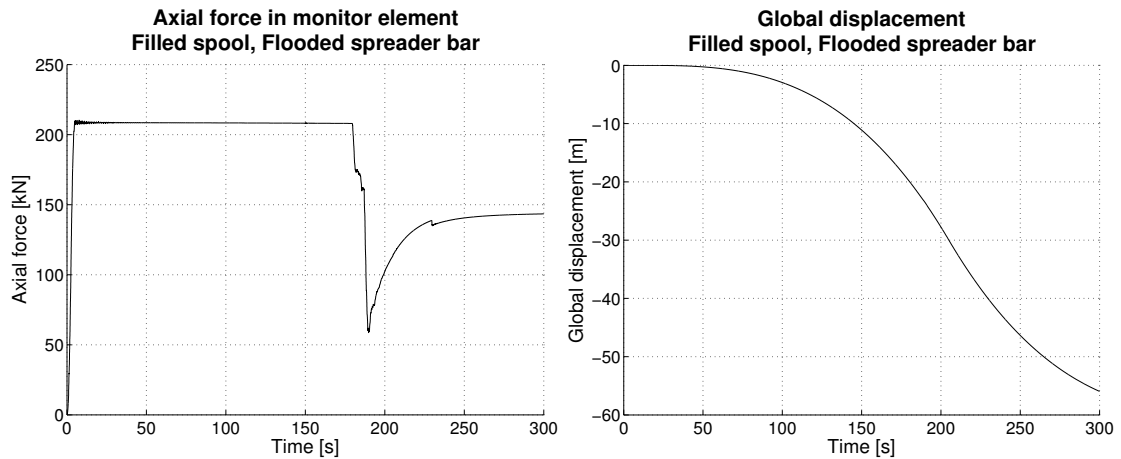
FLOODED          GROUP          2
|
INTFLUID        1024  Drained    30    GROUP    2
|
HydroPar  FloodSw  2  Group  2
|

```

Figure 5.4: Parameters to define drain in the head file. GROUP 2 refers to the spreader bar and its connections to the spool

Figure 5.6 shows how the spool and the spreader bar is filled through the simulation. At the initial time,  $t = 0.01s$  both the spreader and the spool are empty. At  $t = 5s$ , the spool is completely filled with the internal fluid, while the spreader bar is empty. The last figure, at  $t = 262.5$ , verifies that the spreader bar is completely filled with seawater after being submerged.

This is also shown in the plot of the axial force in the wire (see Figure 5.5a). From this it can be observed that the tension force increases as the model is submerged (from  $t = 190s$  to  $t = 300s$ ). This is because the buoyancy force is decreased as the spreader bar is flooded.



(a) Axial force in monitor element (b) Global displacement of the structure

Figure 5.5: Displacement and force in monitor element for filled spool and flooded spreader bar

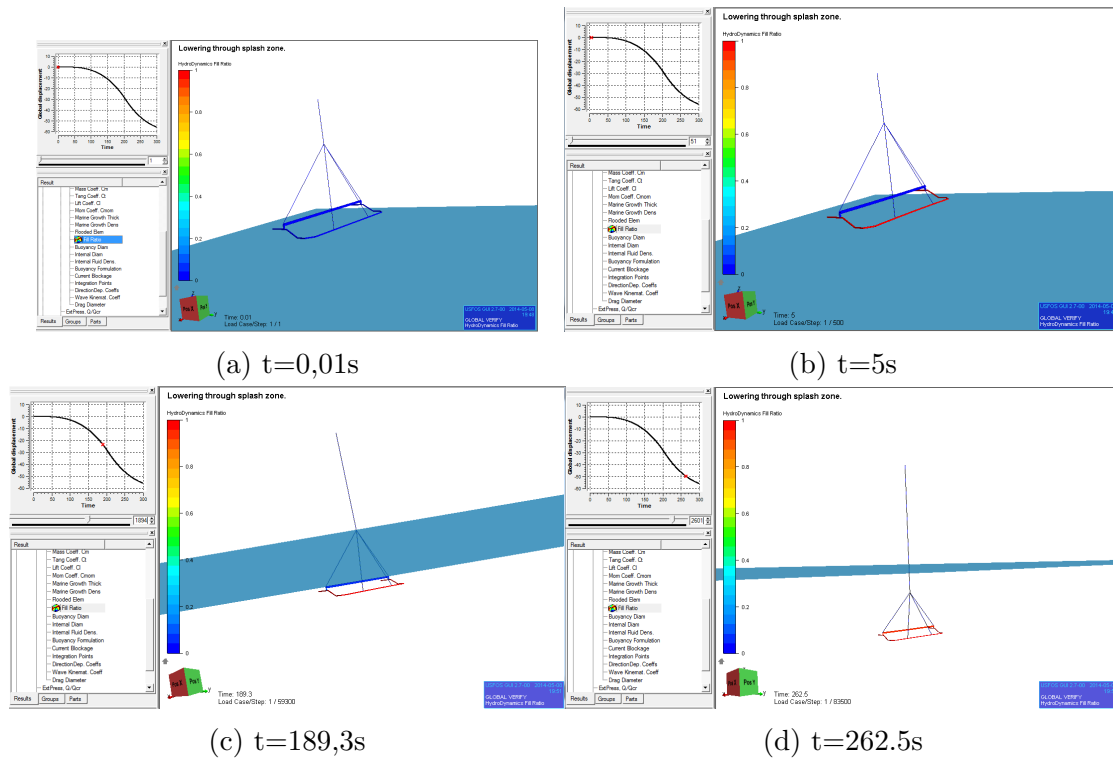


Figure 5.6: Fill ration of spool and spreader bar

### 5.2.4 Verification of equilibrium force in the wire

For the three cases in the previous sections, the equilibrium force in the top of the lifting wire was calculated. The results from these calculations was then compared to the force calculated by USFOS. This was done to get a verification that the weight was calculated in the right way in USFOS in all the cases. Table 5.5 shows the result of these calculation, and the deviation from the USFOS values.

When calculating the equilibrium forces in the wire, static conditions was considered.



Table 5.5: Equilibrium force in the hoisting wire. Comparison between calculated values and USFOS values

<b>Spool</b>	Calculated	USFOS	Diff	Unit
Spool mass	4,99E+03			[kg]
Inner fluid mass	3,94E+03			[kg]
Mass displacement	4,32E+03			[kg]
Weight in air <sup>e</sup>	4,90E+04			[N]
Weight in air <sup>f</sup>	8,76E+04			[N]
Buoyancy force	4,24E+04			[N]
Submerged weight <sup>e</sup>	6,58E+03			[N]
Submerged weight <sup>f</sup>	4,52E+04			[N]
<b>Spreader bar</b>				
Spreader bar mass	1,22E+04			[kg]
Inner seawater mass	9,13E+03			[kg]
Displacement	1,05E+01			[kg]
Weight in air <sup>e</sup>	1,19E+05			[N]
Buoyancy force	1,05E+05			[N]
Submerged weight <sup>e</sup>	1,41E+04			[N]
Submerged weight <sup>f</sup>	1,04E+05			[N]
<b>Total force in wire</b>				
In air <sup>1</sup>	1,68E+05	1,69E+05	8,14E+02	[N]
In Air <sup>2</sup>	2,07E+05	2,08E+05	1,53E+03	[N]
Submerged <sup>1</sup>	2,07E+04	1,43E+04	-6,37E+03	[N]
Submerged <sup>2</sup>	5,94E+04	5,39E+04	-5,47E+03	[N]
Submerged <sup>3</sup>	1,49E+05	1,42E+05	-6,94E+03	[N]

<sup>e</sup> Empty

<sup>f</sup> Filled/Flooded

<sup>1</sup> Empty spool, Empty spreader bar

<sup>2</sup> Filled spool, Empty spreader bar

<sup>3</sup> Filled spool, Flooded spreader bar

From table 5.5, it can be seen that the calculations deviates from the USFOS values. This may be due to several reasons. One of them is that at the time the values are taken from USFOS, the model has a vertical velocity and acceleration. The velocity will lead to a drag force, while acceleration will lead to a mass force and an added mass force. These forces will be according to equation 2.5 and will work against the direction of motion. Thus they will cause a smaller tension force

in the wire, than if the model was at rest. From the table it can be observed that in all the 3 submerged cases the force from USFOS is less than the calculated force. This corresponds to the discussion above.

For the two air cases the USFOS force is larger than the calculated force. However the deviation is smaller for these two air cases than for the submerged cases.

### **5.3 Modeling of slack in USFOS**

Up to this point the slings and the wire are modeled as beam elements. This means that they have capacity in compression as well as tension. In reality they will only have capacity in tension. In other words, if the forces in any of these elements is compressive it will correspond to slack. As discussed in chapter 2.1.6 this can give critical dynamic loads in the wire/slings if the force goes back into tension. The behavior of the model would also be different if the slings and the wire was modeled to take only tension forces.

During the work on thesis it was tested to include this behavior in the model. The thought was to model the slings as non-linear springs instead of beam elements. These springs were defined to have the same stiffness in tension as the original beam elements. However, in compression the non-linear springs was given a stiffness close to zero

This attempt to model slack in USFOS did not give any satisfying results. All the analyses that were run with non-linear springs crashed before they were finished. Therefore, it was continued to use beam elements to model the wire and slings during the rest of this work.

## 5.4 Lowering of spool into regular waves

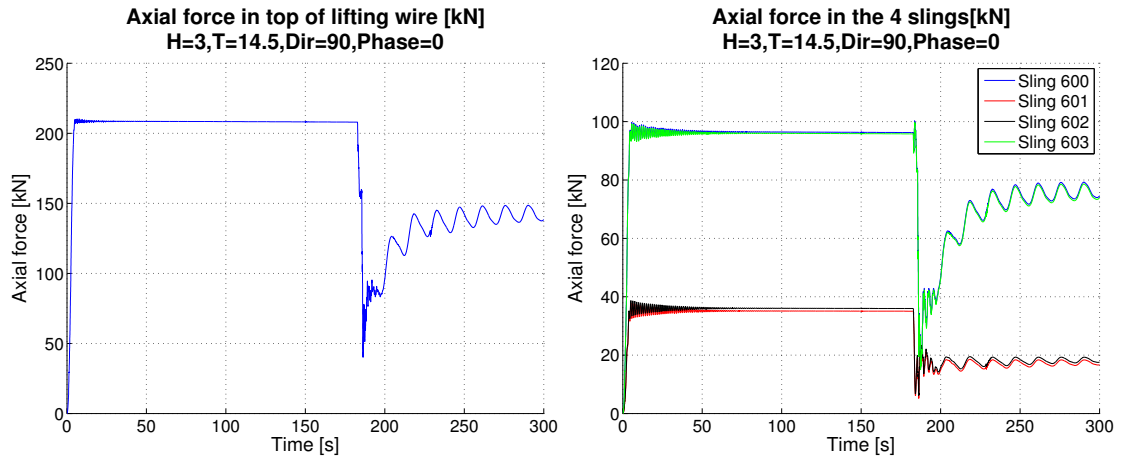
In this chapter, the model used in section 5.2.3, will be used. This was the model where the spool is filled with an internal fluid initially, and the spreader bar is filled with sea water as it is submerged.

Several different cases of waves have been run by using shell scripts. The wave parameters that have been varied are wave heading, wave height and wave period. These parameters were chosen so that they are within the applicability limits of Airy or Stoke's 5th order theory (fig: A.1). The goal of this was to find extreme load cases that may be critical for the structure. The wave heights that are used are large compared to what usually would be operational conditions. But because the top point of the wire still is fixed, these waves will give a less extreme response than if the top of the wire was moving. An overview of the different cases that have been run is given in table 5.6. Each of the cases will be discussed further in this chapter.

Table 5.6: Cases of different wave parameters

Case	Height	Period	Direction	Phase	Theory
1	3	14.5	90	0	Airy
2	6	12.5	90	0	Stokes
3	8	12.5	90	0	Stokes
4	8	8	90	0	Stokes

### 5.4.1 Case 1 - H=3 , T=14.5, Dir=90, Phase=0

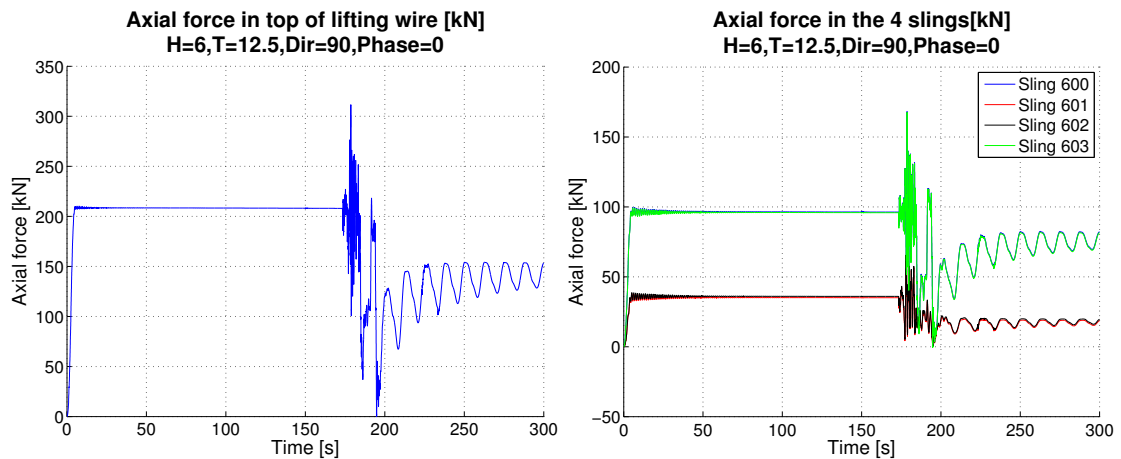


(a) Axial forces in top of the lifting wire. (monitor element)

(b) Axial forces in the 4 slings

Figure 5.7: Axial force in the wire and slings for case 1

### 5.4.2 Case 2 - H=6 , T=12.5, Dir=90, Phase=0

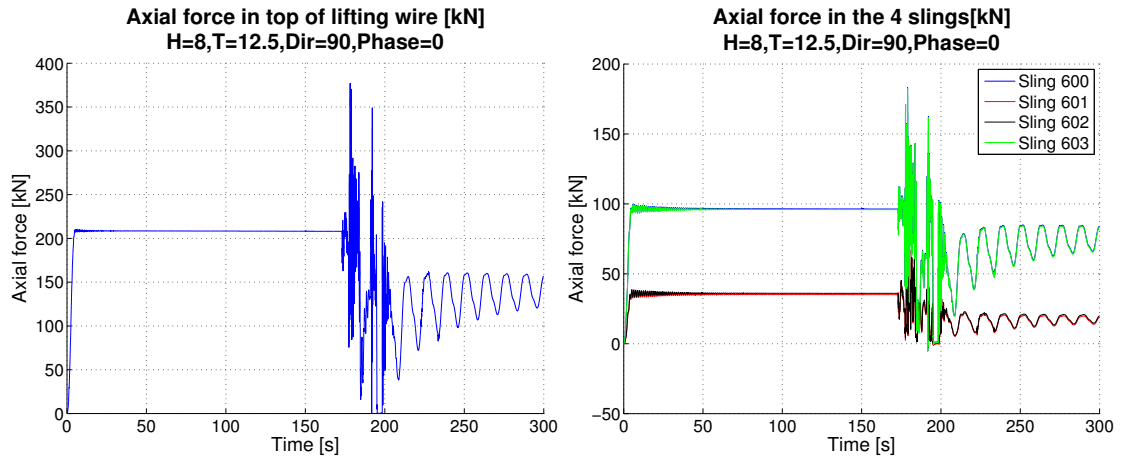


(a) Axial forces in top of the lifting wire. (monitor element)

(b) Axial forces in the 4 slings

Figure 5.8: Axial force in the wire and slings for case 2

### 5.4.3 Case 3 - H=8 , T=12.5, Dir=90, Phase=0

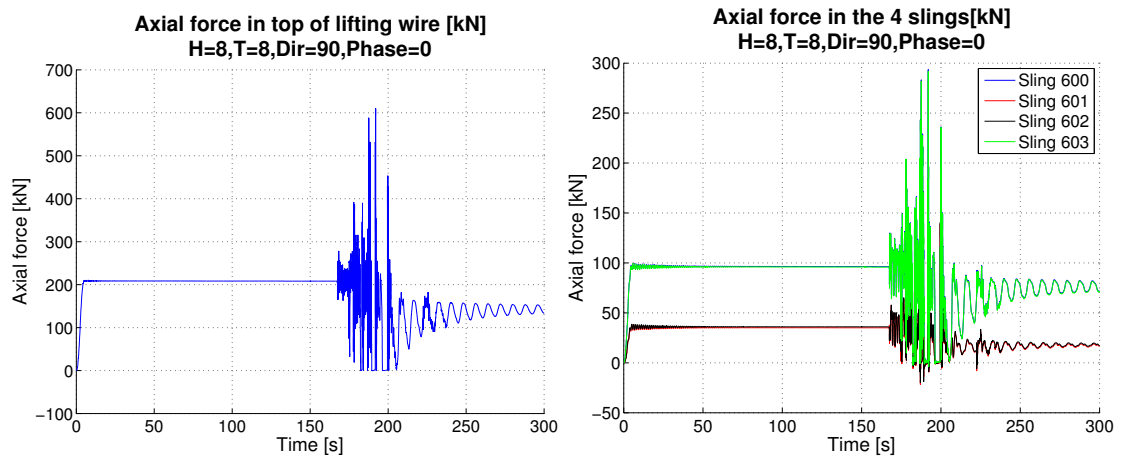


(a) Axial forces in top of the lifting wire.  
(monitor element)

(b) Axial forces in the 4 slings

Figure 5.9: Axial force in the wire and slings for case 3

### 5.4.4 Case 4 - H=8 , T=8, Dir=90, Phase=0



(a) Axial forces in top of the lifting wire.  
(monitor element)

(b) Axial forces in the 4 slings

Figure 5.10: Axial force in the wire and slings for case 4

### 5.4.5 Forces in wire and slings

If we consider the force in the hoisting wire, we can see how the waves affect the response in the wire compared to the case with flat sea (sect: 5.2.3).

In case 1 the axial force in both the wire and all the slings is in tension during the whole lowering process (fig: 5.7b and 5.7a). This means that no slack in the wire or slings will occur for this wave condition. From the figure we can see how the tension force is reduced suddenly as the spool hits the water. Further when the spool is lowered below the splash zone, the tension force increases and approaches the submerged equilibrium force.

For the other 3 cases, the force conditions in the wire and sling becomes more critical. From the plots for case 2 (fig: 5.8b) and 5.7a), it can be observed that the force in the hoisting wire become very close to zero in a short time instant around  $t = 190s$ . This is consistent with the forces in sling 600 and 603. These experience compression around the same time instant.

In addition to a negative force, the plots show that the forces in the wire, sling 600 and sling 603 has large oscillations in the wave zone.

### 5.4.6 Code checking of structural response

In USFOS the structural response histories can be checked with different design codes. In this thesis the API-RP-2A-WSD is used (American Petroleum Institute; 2005). By running the "CodChk" utility tool, the elastic utilization of the model is checked according to this. This program checks the time histories for the model from the start to the end.

When running the program, its standard input parameters are defined. This means that the buckling factor  $K$  is set to be 0.8 and  $\sigma_u/\sigma_y$  is defined to be 1.2. Further mid-node forces are considered. The extreme condition capacity factor is set to be equal to 1.

The max utilization of the spool and spreader bar for the different seastates is presented in table 5.7. The discretization of the spool is shown in appendix D.

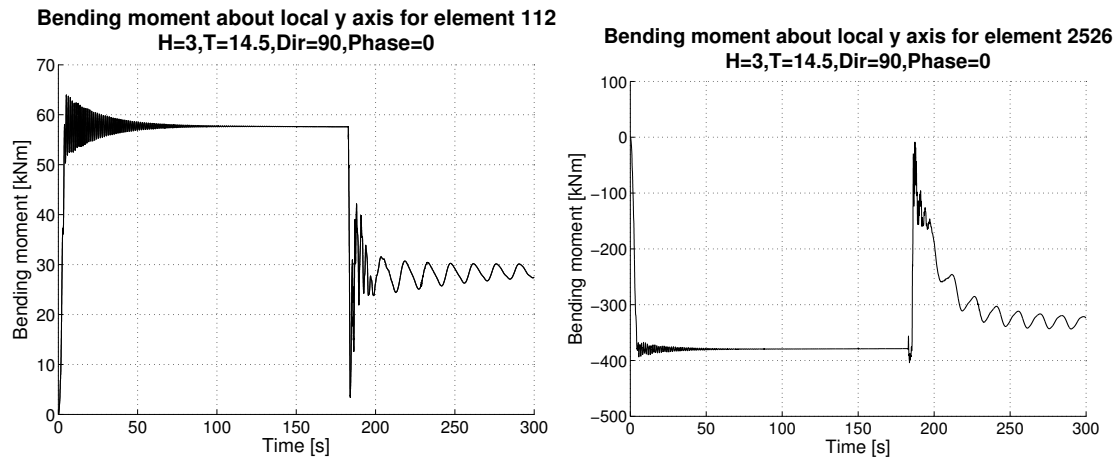
Table 5.7: Elastic utilization according to API WSD

Case	Max	Element ID	Time
1			
<i>Spreader</i>	0.23	2526	183.80
	0.23	2425	183.80
<i>Spool</i>	0.20	23	5.10
	0.20	112	5.10
2			
<i>Spreader</i>	0.40	2526	178.70
	0.40	2425	178.70
<i>Spool</i>	0.40	1415	178.00
	0.40	45	178.00
3			
<i>Spreader</i>	0.50	2526	179.00
	0.50	2425	179.00
<i>Spool</i>	0.45	112	179.70
	0.44	12	179.70
4			
<i>Spreader</i>	0.59	2526	187.70
	0.59	2425	187.70
<i>Spool</i>	0.76	112	192.10
	0.74	12	192.10

From table 5.7 it can be observed that the elastic utilization of the structure is lowest for the first case and increases from case 1 to case 4.

The table also shows at which time the maximum utilization occurs. The maximum value for the spreader bar always seem to occur when the structure is in the splash zone. This is also the case for the spool, except for the first seastate, where the time is 5.1 seconds. However, this utilization value is due to the initial phase where gravity is turned on (from  $t = 0s$  to  $t = 5s$ ) and the spool is filled (from  $t = 0s$  to  $t = 1s$ ). The forces in the structure oscillates about the equilibrium values in air due to this initial phase. These oscillations will not be present in reality and thus these initial oscillations should be neglected when considering the structural response.

Examples of this is shown in figure 5.11 where the bending moment about the local y axis for element 2526 and 112 is plotted. For element 112 it can be observed that there are large oscillations initially, and that this leads to the highest bending moment of the time history (see Figure 5.11a). This corresponds to the time where the maximum elastic utilization is found (see Table 5.7).



(a) Bending moment about local y axis for element 112 (b) Bending moment about local y axis for element 2526

Figure 5.11: Bending moment about local y axis

If figure 5.11b is studied, it can be seen that the maximum value of the bending moment for element 2526 is at  $t = 183.8s$ . This is also the time instant where the elastic utilization for the spreader bar reaches its maximum value (see Table 5.7).



# 6 Lowering of a subsea spool into irregular waves

In order to make the simulations more realistic, it is necessary to model the sea state with irregular waves. In addition to this the top of the lifting wire should be connected to a moving crane-tip instead of being fixed. This chapter will take these factors into account when simulating lowering through the splash zone. The structural response of the wire, slings, spool and spreader will be considered.

## 6.1 Model

The model considered in this chapter consist of the following parts:

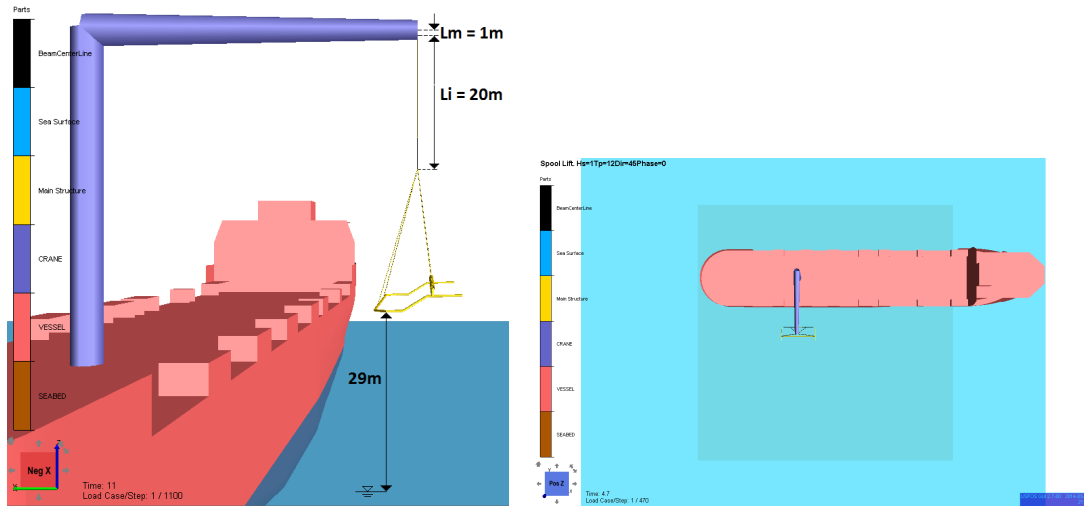
- A subsea spool and spreader bar (same as in chapter5)
- A crane model
- A vessel model

The same spool model as in the previous chapter is used. This is the model where the spool is filled initially, and the spreader bar is flooded with sea water when it is submerged. The difference lies in how the top of the wire is defined and the initial length of the wire. It is set to have twice the initial length compared to earlier, which implies that it has half the initial stiffness. Additionally it is not fixed as earlier, but attached to a moving crane tip. This will make the model more realistic.

The crane is connected to a horizontal beam element that has motions in all 6 degrees of freedom described by RAO functions. These functions are shown in Appendix B. They are defined from a period of 3 seconds to 25 seconds.

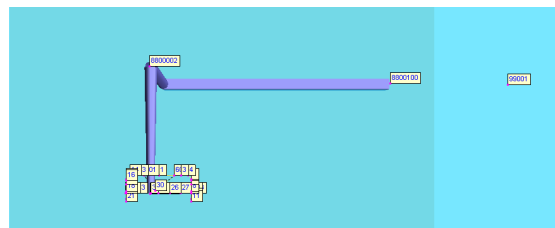
The crane and beam elements are also connected to a vessel model. However, the model of the vessel does not contribute to the motions of the system. This is just for visualization purposes.

The RAO's that are used are defined to be the same in all directions. This would usually not be the case for a real vessel. I.e if the wave heading is zero degrees (propagating in positive x direction) the vessel should have different response in roll or sway, than if the wave heading was 90 degrees (propagating in positive y direction). However, the RAO's that are used seem reasonable for wave headings of 45 degrees.



(a) Model dimensions.  $L_i$  is the initial length of the lifting wire.  $L_m$  is the length of the "monitor" element. The initial height above the sea surface is also indicated.

(b) Model in the xy plane



(c) Crane and beam elements in the xy plane

Figure 6.1: Model description

## 6.2 Cases of irregular waves

To model the irregular waves, the JONSWAP wave spectrum have been used. The wave periods of the spectrum have been defined to range from 3 seconds to 25 seconds. Many different cases of significant waveheight,  $H_s$ , and peak period,  $T_p$  have been run. Different wave headings have also been simulated. Table 6.1 give an overview of the different cases.

Table 6.1: Cases of irregular waves with 45 degree heading

Significant wave height, $H_s$	Spectral peak period, $T_p$							
	4 s	6 s	8 s	10 s	12 s	14 s	16 s	18 s
0.5 m	x	x	x	x	x	x	x	x
1 m	x	x	x	x	x	x	x	x
2 m	x	x	x	x	x	x	x	x
3 m	x	x	x	x	x	x	x	x
4 m	-	x	x	x	x	x	x	x
5 m	-	x	x	x	x	x	x	x

x: Case have been run

-: Case have not been run

### 6.3 Minimum forces in the wire and slings

During a lifting operation the forces in the wire and slings should remain in tension at all times. This is to avoid slack in wires/slings followed by high snap loads (see Section:2.1.6). As mentioned earlier, the simplified method of DNV (2011), recommends that the tension force in the should not be less than 10% of the submerged weight.

The time-histories for the wire and sling forces have been studied. For each case of significant wave height and spectral peak period, the minimum force in the is found. The minimum point is found in the time range,  $t \in [80, 320]$ , so that the force in the initial phase is neglected. The results are shown in figure 6.2 to 6.6.

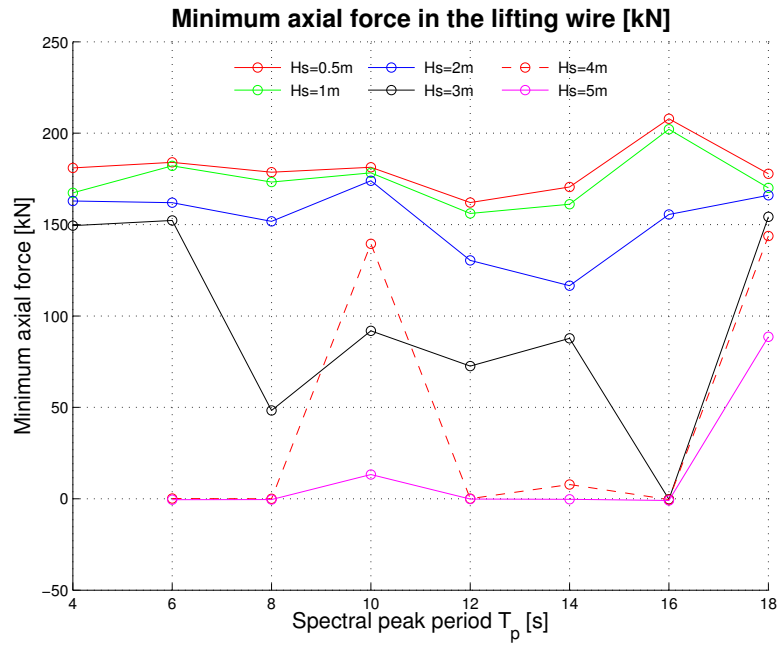


Figure 6.2: Minimum axial force in the lifting wire

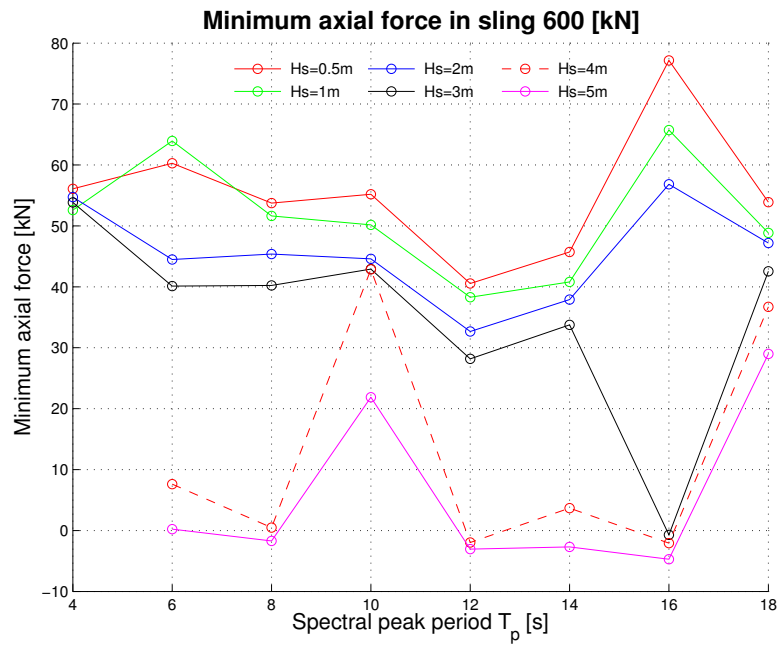


Figure 6.3: Minimum axial force in sling 600

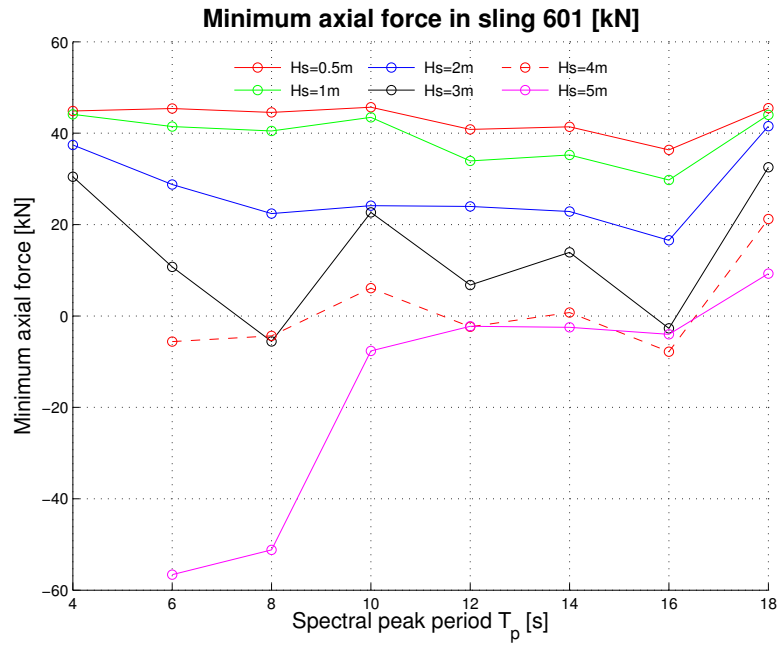


Figure 6.4: Minimum axial force in sling 601

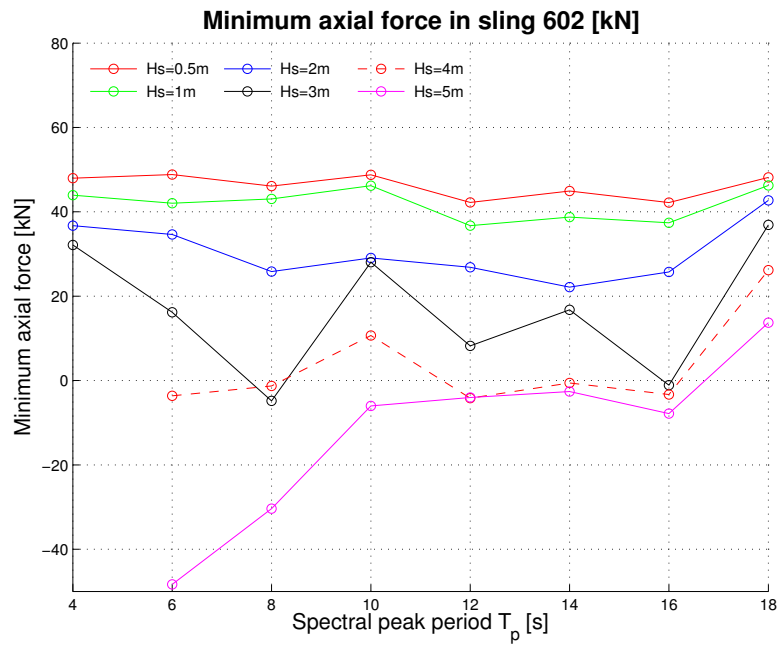


Figure 6.5: Minimum axial force in sling 602

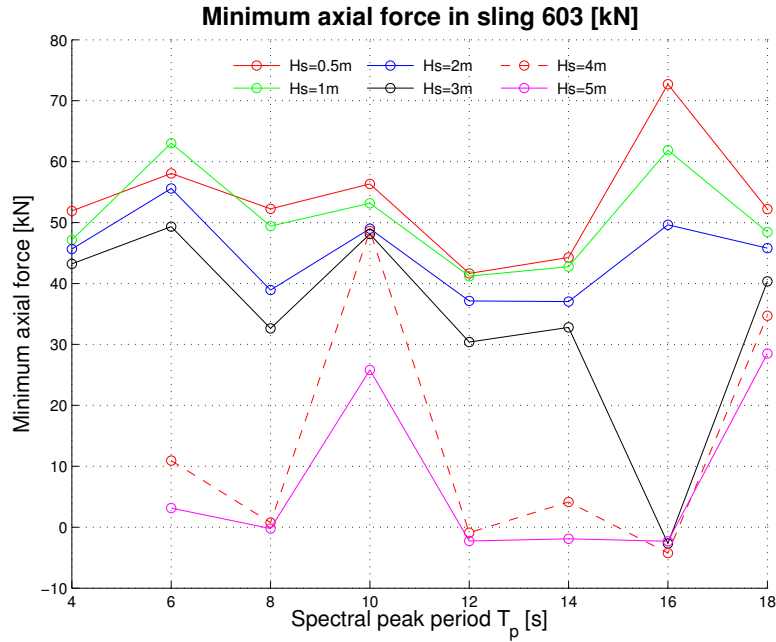


Figure 6.6: Minimum axial force in sling 603

### 6.3.1 Discussion of results

#### Lifting wire

Figures 6.2 to 6.6 shows the minimum force in the lifting wire for different cases of  $T_p$  and  $H_s$ .

For the lifting wire it can be observed that the minimum force decreases as the significant waveheight increases. This is true for all values of  $H_s$  except for the case when  $H_s = 4m$  and  $T_p = 10s$ .

The minimum force in the wire does not go below zero for the first three cases of significant waveheights. This means that neither the wire or the slings will be slack in these cases. For the three remaining cases this not the case. When the spectral peak period is equal to 16 seconds, the wire force becomes less than zero for  $H_s = 3m, 4m, 5m$ . Additionally the force is zero at several other values of  $T_s$  for the two latter cases. This implies that the wire will go slack for these cases and that large snap loads can be present. This can again become critical for the operation.

If the limiting force in the wire is set to be 10 percent of the submerged weight,

the minimum force will be about 14.2 kN. From figure 6.2 it can be observed that this will make two additional seastates critical ( $H_s = 4m, T_p = 14s$  and  $H_s = 5m, T_p = 10s$ ).

It should be noticed that the present model in USFOS does not describe the slack condition physically correct. This is because the slings have capacity in compression. Thus if compressive forces do occur in the wire or slings, the behavior of the model will be incorrect. However, knowing that a given seastate can lead to slack wire and/or slings, will be determining when defining the limiting seastates for an operation.

### Slings

Considering the minimum forces in the four slings (fig: 6.2-6.6), the same trend as for the lifting wire can be observed (with a few exceptions). Also for these elements, the three seastates with highest value of significant wave height ( $H_s = 3m - 5m$ ), are critical when it comes to slack condition. The two slings that are connected to the spreader bar become slack in 7 of the seastates. Sling 601 and 602 experience slack condition for the same 7 seastates plus an additional 5 and 6, respectively.

## 6.4 Maximum force in lifting wire - dynamic amplification factor

The maximum force in top of the lifting wire have been considered. This will be determining when designing the lifting equipment. The dynamic amplification factor is for each of the cases is found by dividing the maximum dynamic force in the lifting wire by the static weight of the structure. For each case, the static weight from USFOS is used (see Table 5.5). The maximum dynamic amplification factor,  $DAF_{max}$ , is calculated according to equation 6.1.

$$DAF_{max} = \frac{F_{max}(t)}{W_0} \quad (6.1)$$

where,

- $F_{max}$  = maximum dynamic force in a time series [N]
- $DAF_{max}$  = maximum value of the dynamic amplification factor in a time series [-]
- $W_0$  = weight of object in air [N]

Table 6.2: Dynamic amplification factors for the different seastates

Significant wave height, $H_s$	Spectral peak period, $T_p$	4 s	6 s	8 s	10 s	12 s	14 s	16 s	18 s
	0.5 m		3.1	3.1	3.1	3.1	3.1	3.1	3
1 m		3.1	3.1	3.1	3.1	3.1	3.1	3.1	3.1
2 m		3.1	3.2	3.2	3.2	3.2	3.1	3.1	3.1
3 m		3.2	3.2	4.2	3.9	3.3	3.2	3.2	3.1
4 m		-	3.4	4.3	3.7	4.2	3.3	3.3	3.2
5 m		-	4.7	4.5	4.6	3.7	3.6	3.5	3.2

- Case have not been run

From table 6.2 it can be observed that the DAF ranges from 3 to 4.7. These are, in general, high values for the dynamic amplification. Thus it should be questioned if the high maximum values found from USFOS is realistic or not. The high values can possibly be due to numerical error in the analyses. In addition the hydrodynamic calculation may not be applicable for the irregular sea state that is modeled.



## 7 Conclusion

In this thesis work USFOS has been used to model marine lifting operations. The focus was put on lowering of objects through the splash zone. The following cases have been studied:

- A straight horizontal pipe with two lifting wires. The wires was fixed in the top end
- A subsea spool connected to 4 slings and a lifting wire. The lifting wire was fixed in top end
- A subsea spool connected to 4 slings and a lifting wire. The top end of the lifting wire was connected to a moving crane tip.

For each of these three main cases, several variations were run. For the first case, the focus was put on how USFOS could be used to model marine lifting operations. The forces in the lifting wires were considered. These elements were modeled as tension springs using a special beam formulation available in USFOS. In order to check if USFOS calculated the force in the wire elements right, the top of each of them were connected to a short beam element ("monitor" element). From this it was found that USFOS calculated the equilibrium forces in the wires correctly, if zero damping was introduced to the system. However when damping was used, the forces in the monitor and wire element was different. This difference results from a certain energy loss due to damping, as the wire-length is increased.

In addition to this it was studied how different input parameters affected the results. It was found that if the incremental change in the lifting wire length was too large, its axial force would go to zero in that time step.

In the second case the lowering of a subsea spool into flat sea and regular waves were simulated. Also, for this case, the lifting wire was connected to a "monitor" element that was fixed in the top. The results from the flat sea states showed that USFOS could be used to model that the subsea spool was filled with an internal fluid initially. Additionally the spreader bar was flooded as it was submerged. Weight calculations was carried out to get a verification that this worked properly. The results from these calculations was different from the USFOS results. A conclusion that can be drawn from this is that the model works properly and that the difference is due to simplifications in the calculations, and the fact that the force values from USFOS were affected by damping, hydrodynamic loads and inertia.

When lowering of the spool into regular waves, the axial forces in the lifting slings

and the top of the wire was considered. It was shown that the slack condition of these occurred in 3 out of 4 cases. Further code checking according to API-RP-2A-WSD was also carried out. This showed that the elastic utilization of the structure was below 1 for all of the cases, but increased as the waves got higher. The highest utilization factor was in the splash zone for all the cases with one exception. For this, the maximum utilization was found initially, after the gravity was introduced. In the time after this phase, oscillations are present. These oscillations are not realistic, and therefore the initial phase should be neglected when considering utilization of the lowered structure.

There are several uncertainties in the code checking that was performed. One of these is the buckling factor of 0.8 that was used. It can be questioned how realistic this is for the present model.

For the last case that was studied, the top of the lifting wire was moving according to defined RAO functions. Different irregular sea states was modeled. For these sea states the minimum force in the wire, was considered. The trend showed that, as  $H_s$  was increased, the wire force decreased. This gave an idea of which sea states that could lead to slack wire and slings.

For the irregular wave model, the maximum wire force and dynamic amplification were also considered. The values for the dynamic amplification was shown to be relatively high. Therefore it is questioned how accurate the force results in USFOS are in the splash zone.

The different models that have been investigated, shows that USFOS can be used to model simple marine lifting operations. The program seem to model the dynamic behavior of the structure in a realistic way. USFOS also calculates the dynamic equilibrium force in the monitor element in the right way. However, for the wire element, the equilibrium force is reduced in each time step if damping is introduced to the system.

The programs applicability for modeling marine lifting operations, is limited in several ways. The lowered structure must consist of cylindrical members for the hydrodynamic calculation to work properly. These calculations are also very simplified. Additionally it should be made possible to initiate the dynamic analysis with a static analysis. In this way oscillations due to initiation of gravity would be avoided. It is not known to the author that this is possible when the special beam formulation is used

## 8 Suggestions for further work

During the thesis work the initial scope was reduced. Therefore it is recommended that further work on the topic includes the scope that was neglected here. Especially comparing the USFOS results to the results from alternative software such as SIMO, would be interesting. This could give a better insight in the applicability of USFOS to model marine lifting operations, and improvements that could be made.

Further work should also include a more thorough simulation of irregular sea states, using more realistic RAO functions and vary the wave heading. Varying the seed number for the irregular waves and building a statistical model for the response, would also be of interest.

In this thesis it was tested if the wires and slings could be modeled as non-linear springs, so that their capacity in compression was zero. The thought behind this was to model the dynamic behavior when the wires and slings became slack. However this study did not lead to any good results. Nonetheless a more thorough study on this could be performed.

This thesis covered lowering through the splash zone. If further work is to be carried out, it can also use USFOS to analyze other phases of a lifting operation. I.e looking at the structural response during landing on the seabed. Thus the applicability of the program for modeling this phase could be evaluated.



## 9 Bibliography

- Alvær, P. Ø. (2012). the VMO Standard & ISO 19001 Marine Operations, *2nd Marine Operations Speciality Symposium (MOSS 2012)*.
- American Institute of Steel Construction inc. (2005). *Steel Construction Manual*, 13th edn.
- American Petroleum Institute (2005). Recommended Practice for Planning , Designing and Constructing Fixed Offshore Platforms — Working Stress Design, (October 2005).
- Araujo, R., Vaz, M. A. and Couto, P. (2012). Methodology for Overboarding Operations, *2nd Marine Operations Speciality Symposium*, pp. 325–336.
- Bai, Y. and Bai, Q. (2012). Installation and Vessels, *Subsea Engineering Handbook*, Elsevier Inc., chapter 5, pp. 139–158.
- Campbell, I. and Weynberg, P. (1980). Measurements of Parameters Affecting Slamming, *Technical report*.
- DNV (2011). Modelling And Analysis Of Marine Operations, *Recommended Practice, DNV-RP-H103* .
- Faltinsen, O. M. (1990). *Sea Loads On Ships And Offshore Structures*, Cambridge University Press.
- Gordon, R. B., Grytø yr, G. and Dhaigude, M. (2014). Modeling of Suction Pile Through the Splash zone, *Proceedings of the ASME 2013 32nd International Conference on Ocean, Offshore and Arctic Engineering*, Nantes, France, pp. 1–9.
- Greco, M. (2012). TMR 4215 : Sea Loads Lecture notes.
- Holmås, T. (2010). Release Notes USFOS 8-5.  
**URL:** *www.usfos.com*
- Nielsen, F. G. (2007). *Lecture Notes In Marine Operations*, Department of Marine Hydrodynamics, Trondheim/Bergen.
- Parimi, M. and Qian, Z. (2008). Installation of large Suction Piles in the Gulf of Mexico.
- Sandvik, P. C. (2007). Theory Related To Subsea Lifting Operations, *Presentation*, Stavanger.

Sarkar, A. and Gudmestad, O. T. (2010). Splash zone lifting analysis of subsea structures, *Proceedings of the ASME 2010 29th International Conference on Ocean, Offshore and Arctic Engineering*, Shanghai, China.

SINTEF Group (2001). USFOS Getting Started.

**URL:** *www.usfos.com*

Søfteland, T. E. (1990). *Lifting analysis of integrated spool cover*, Master thesis, University of Stavanger.

Thiagarajan, K. P., Yann, N., Stena, C. and Asia, O. (2001). OTC 13242 Assessment of One Company ' s Regulations for Offshore Lifting Operations.

Thurston, K. W., Swanson, R. C. and Kopp, F. (2014). Statistical Characterization of Slacking and Snap Loading During Offshore Lifting and Lowering in a Wave Environment, *Proceedings of the ASME 2011 30th International Conference on Ocean, Offshore and Arctic Engineering*, pp. 1–9.

Usfos As (2010). USFOS - Hydrodynamics.

**URL:** *www.usfos.com*

Usfos As (2014). USFOS User's Manual - Input Description USFOS Control Parameters.

**URL:** *www.usfos.com*

# Appendices





# A Wave theory applicability

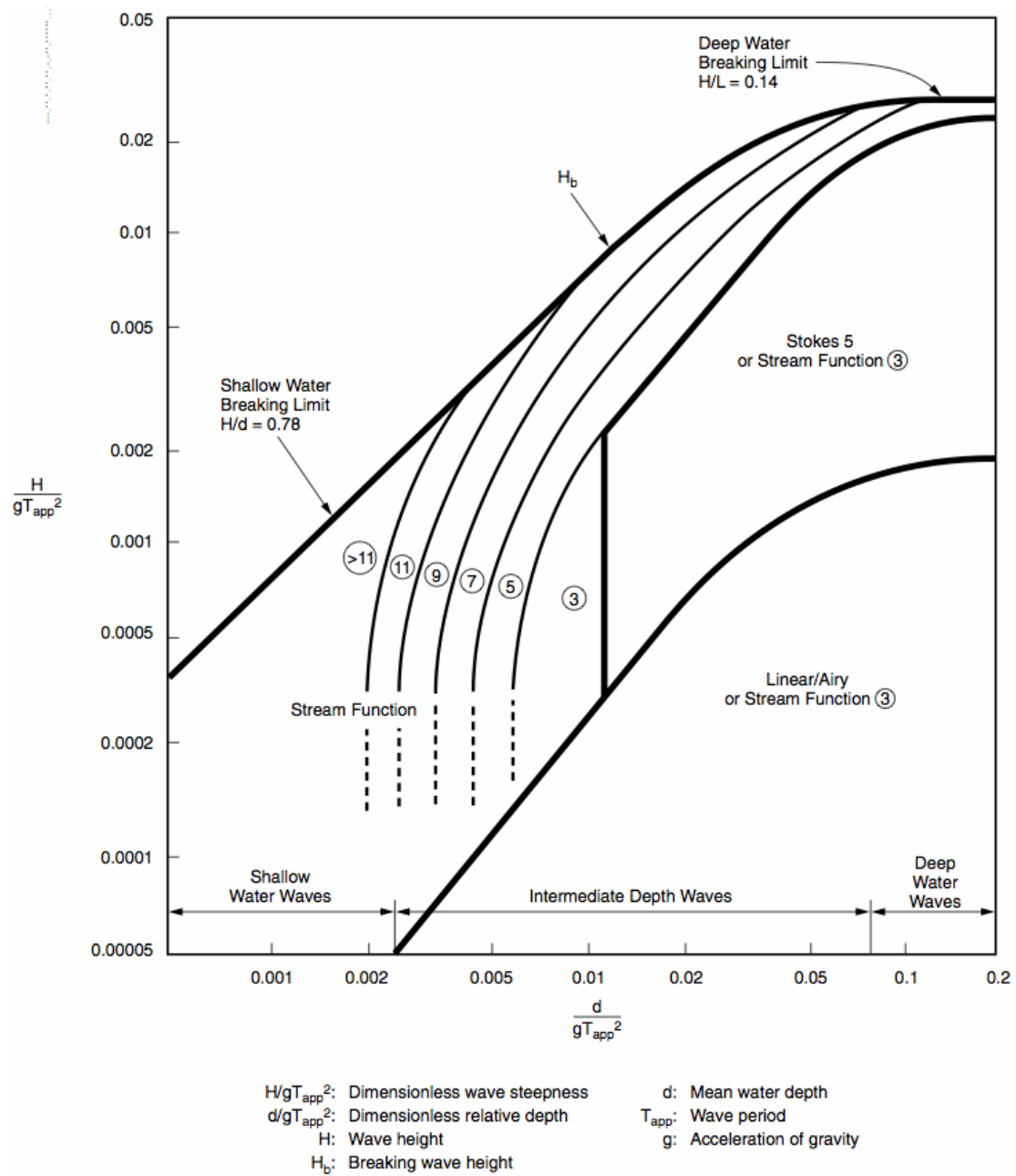


Figure A.1: Wave theory applicability (American Petroleum Institute; 2005)



# B RAO functions

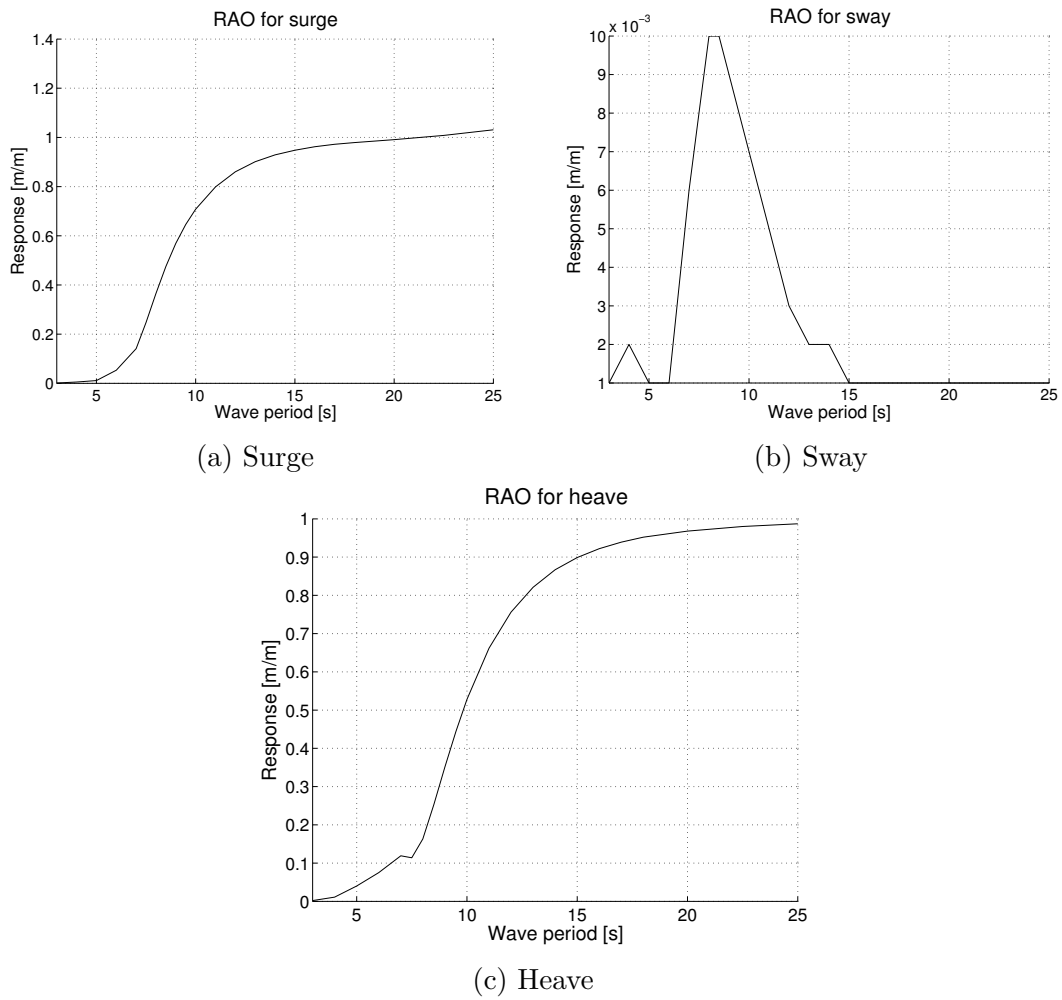
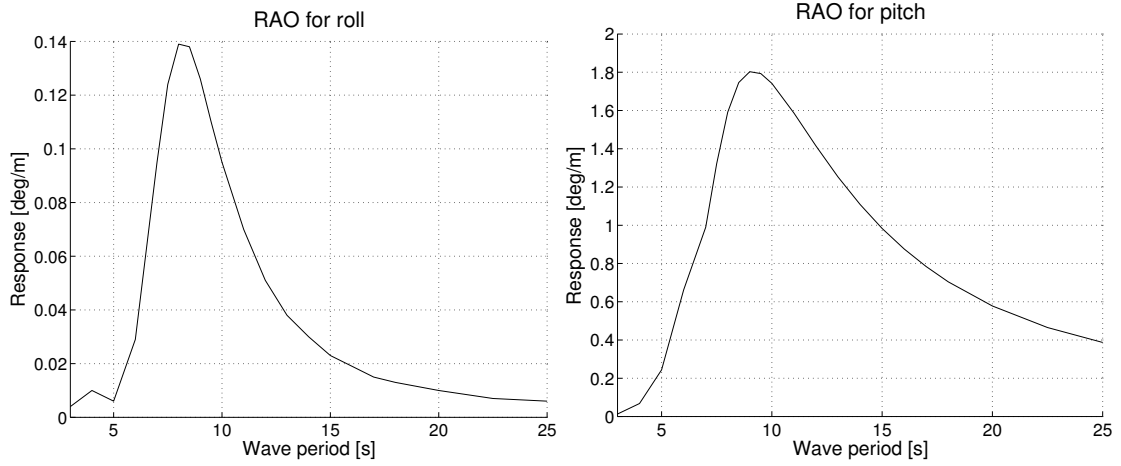
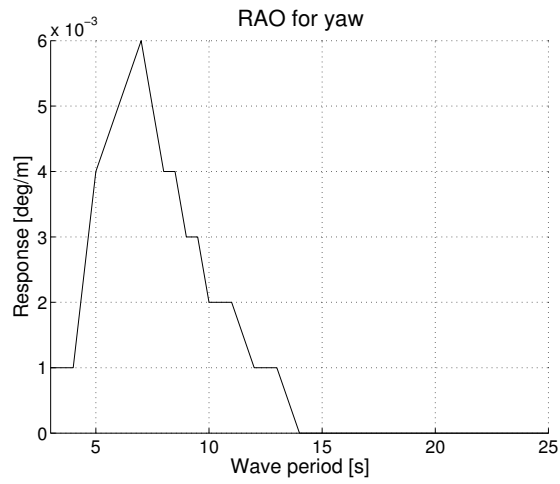


Figure B.1: RAO for surge, sway and heave



(a) Roll

(b) Pitch



(c) Yaw

Figure B.2: RAO for roll, pitch and yaw

# C Buckling factor for idealized boundary conditions







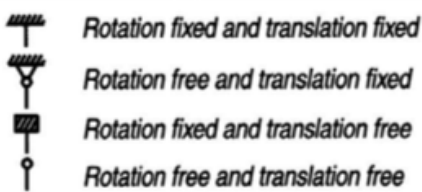
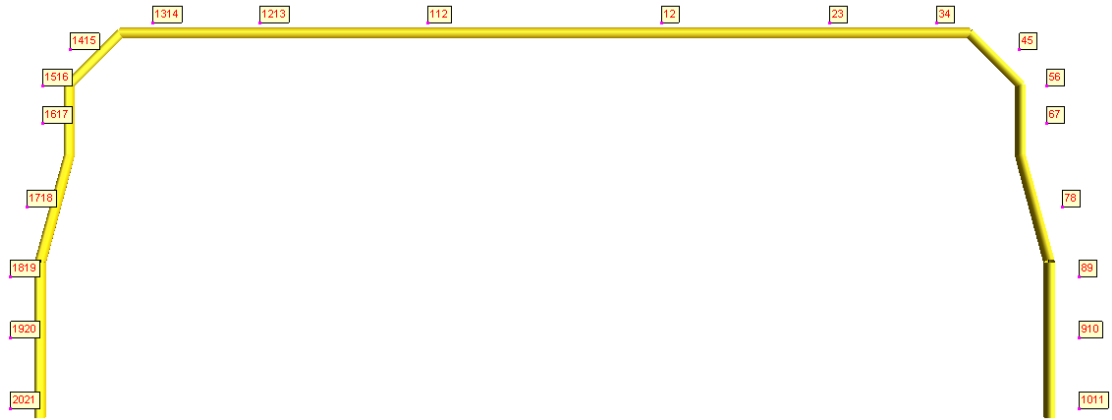
TABLE C-C2.2 Approximate Values of Effective Length Factor, $K$						
Buckled shape of column is shown by dashed line.	(a) 	(b) 	(c) 	(d) 	(e) 	(f) 
Theoretical $K$ value	0.5	0.7	1.0	1.0	2.0	2.0
Recommended design value when ideal conditions are approximated	0.65	0.80	1.2	1.0	2.10	2.0
End condition code						

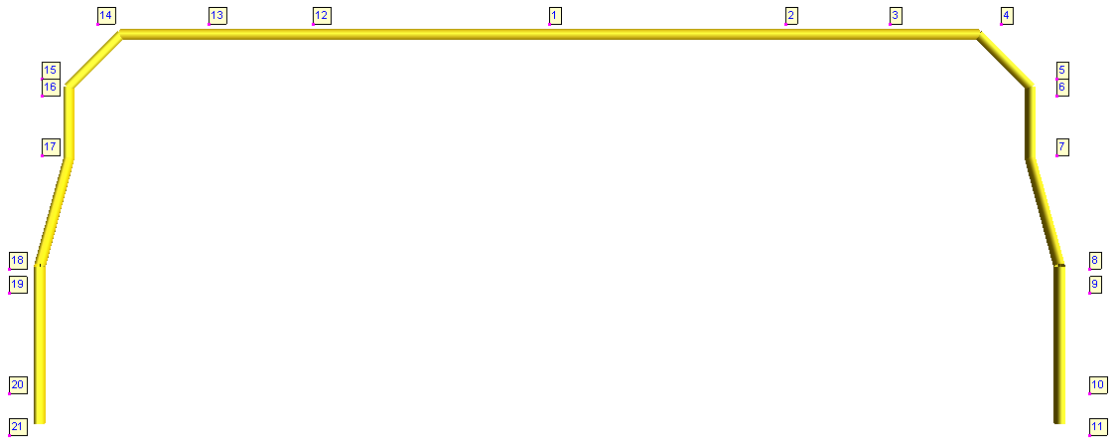
Figure C.1: Buckling factors for idealized boundary conditions (American Institute of Steel Construction inc.; 2005)



# D Discretization of spool model



(a) Element numbers for the spool

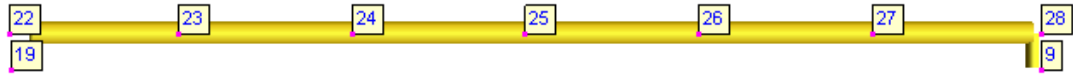


(b) Node numbers for the spool

Figure D.1: Discretization of the spool



(a) Element numbers for the spreader bar



(b) Node numbers for the spreader bar

Figure D.2: Discretization of the spreader bar